

12-1-1996

# Temporal Characteristics of Zebrafish Cone Types and Their Role in Separate Visual Processing

Warren Patterson

*Western Kentucky University*

Follow this and additional works at: <http://digitalcommons.wku.edu/theses>



Part of the [Psychology Commons](#)

---

## Recommended Citation

Patterson, Warren, "Temporal Characteristics of Zebrafish Cone Types and Their Role in Separate Visual Processing" (1996). *Masters Theses & Specialist Projects*. Paper 879.  
<http://digitalcommons.wku.edu/theses/879>

This Thesis is brought to you for free and open access by TopSCHOLAR®. It has been accepted for inclusion in Masters Theses & Specialist Projects by an authorized administrator of TopSCHOLAR®. For more information, please contact [connie.foster@wku.edu](mailto:connie.foster@wku.edu).

TEMPORAL CHARACTERISTICS OF ZEBRAFISH CONE TYPES  
AND THEIR ROLE IN SEPARATE VISUAL PROCESSING

A Thesis

Presented to

the Faculty of the Department of Psychology

Western Kentucky University

Bowling Green, Kentucky

In Partial Fulfillment

of the Requirements for the Degree

Master of Arts

by

Warren Frederick Patterson, II

December 1996



TEMPORAL CHARACTERISTICS OF ZEBRAFISH CONE TYPES  
AND THEIR ROLE IN SEPARATE VISUAL PROCESSING

Date Recommended August 1, 1996

Joseph Bitt

Director of Thesis

Karlene Ball

Shawn Muttu

Elmer Gray 10/31/96

Dean, Graduate Studies and Research Date

## Acknowledgements

I would like to thank the members of my committee, Drs. Joseph Bilotta, Karlene Ball, and Sharon Mutter for all of their assistance and patience in completing this thesis. A special thanks is owed to Dr. Bilotta for the countless hours he spent designing and building the optical system and running fish as well as for his efforts as a first-rate mentor. I also want to thank R. Alan Hughes for being a great friend and a sounding board for my problems and ideas. Finally, I especially want to thank my wife, Emily, for all of the love and patience shown toward me while I completed this thesis. She has always been my best friend and I could ask for nothing more from her. I also appreciate all of the time she sacrificed so that I could use the computer. This project was supported by KY NSF/EPSCoR grant OSR-94-52-895 and a grant from the Western Kentucky University Office of Graduate Studies and Research. Thanks also to Dr. Karlene Ball and Dr. Paul DeMarco for the loan of equipment to complete our recording.

## Table of Contents

|  | <u>Page</u> |
|--|-------------|
| Acknowledgements.....  | iii         |
| List of Figures.....   | v           |
| Abstract.....  | vi          |
| Chapter 1: Introduction.....                                     | 3           |
| Chapter 2: Review of the Literature                              |             |
| Overview.....  | 6           |
| Optics of the Eye.....   | 7           |
| Anatomy and Physiology of the Eye.....                           | 7           |
| Requirements for Color Vision.....                               | 12          |
| Theories of Color Vision.....                                    | 14          |
| Anatomical Separation of Visual Processing Pathways.....         | 18          |
| Using HFP to Determine the Cone Inputs to Separate Channels..... | 25          |
| Zebrafish Model.....   | 27          |
| Summary.....   | 29          |
| Chapter 3: Method  |             |
| Participants.....  | 31          |
| Apparatus.....   | 31          |
| Procedure.....   | 34          |
| Chapter 4: Results.....  | 38          |
| Chapter 5: Discussion.....                                       | 51          |
| References.....  | 62          |
| Table 1.....   | 68          |
| Figure Captions.....   | 69          |
| Appendix.....  | 93          |

## List of Figures

| <u>Figure</u>  | <u>Page</u> |
|--|-------------|
| 1. Absorptance Spectra of the Zebrafish Visual System.....                   | 73          |
| 2. Unfiltered ERGs to 4.6 Hz and 16 Hz Stimuli.....                          | 74          |
| 3. Filtered ERGs to 4.6 Hz and 16 Hz stimuli.....                            | 75          |
| 4. One-Thousand ms Segment of Filtered ERG to 16 Hz Stimuli.....             | 76          |
| 5. Averaged ERGs to 4.6 Hz and 16 Hz Stimuli.....                            | 77          |
| 6. Three ERG Responses to 4.6 Hz Stimuli.....                                | 78          |
| 7. Irradiance Response Function to 4.6 Hz 420 nm Stimuli.....                | 79          |
| 8. Irradiance Response Function to 16 Hz 520 nm Stimuli.....                 | 80          |
| 9. Irradiance Response Function with Isoluminant Point.....                  | 81          |
| 10. Irradiance Response Function with False Isoluminant Point.....           | 82          |
| 11. Multiple Irradiance Response Functions to 4.6 Hz Stimuli.....            | 83          |
| 12. Spectral Sensitivity Function for Individual Subject.....                | 84          |
| 13. Averaged Spectral Sensitivity Function to 4.6 Hz Stimuli.....            | 85          |
| 14. Averaged Spectral Sensitivity Function to 16 Hz Stimuli.....             | 86          |
| 15. Averaged Spectral Sensitivity Functions to 4.6 and 16 Hz Stimuli.....    | 87          |
| 16. Modeled and Actual Spectral Sensitivity Functions to 4.6 Hz Stimuli..... | 88          |
| 17. Modeled and Actual Spectral Sensitivity Functions to 16 Hz Stimuli.....  | 89          |
| 18. Temporal Response Function of Four Cone Types.....                       | 90          |
| 19. Temporal Frequency Responses of Four Cone Types.....                     | 91          |
| 20. Response Suppression to Chromatic Adaptation.....                        | 92          |

TEMPORAL CHARACTERISTICS OF ZEBRAFISH CONE TYPES  
AND THEIR ROLE IN SEPARATE VISUAL PROCESSING

Warren Frederick Patterson, II

December, 1996

93 Pages

Directed by: Joseph Bilotta, Ph.D., Karlene Ball, Ph.D., and Sharon Mutter, Ph.D.

Department of Psychology

Western Kentucky University

Chromatic and luminance information are processed separately by the visual systems of most higher vertebrates via anatomically separate pathways. Research on primates suggests that the luminance mechanism transmits information about stimulus luminance, movement, and flicker while chromatic mechanisms signal color and detailed information. In order to signal rapid movement, the luminance channel transmits information more rapidly than the chromatic mechanism. While some lower vertebrates such as the zebrafish (*Danio rerio*) do not demonstrate anatomical separation of processing, it is believed that separate processing is a basic requirement of vertebrate vision. The spectral sensitivity functions (relative sensitivity to different wavelengths of light) of the separate mechanisms were determined in zebrafish using heterochromatic flicker photometry (HFP). The spectral sensitivity function of the luminance channel was determined using a flicker rate of 16 Hz which assessed its rapid response rate while the chromatic channel was stimulated with 4.6 Hz flicker. The electrical responses of the

visual system to the HFP stimuli were measured by the electroretinogram. The spectral sensitivity functions of the two channels were modeled by a nonlinear regression equation to assess the relative contributions of each cone type to the spectral sensitivity functions of the two channels. In addition, the temporal resolution of the four cone types was assessed to determine if the temporal response rates of the cone types are responsible for the determination of the channels to which the cones contribute. The spectral sensitivity functions determined by HFP showed no significant difference between the two temporal rates suggesting that zebrafish do not have separate channels for the processing of color and luminance information. In addition, the cone contribution modeling showed no opponency characteristic of chromatic processing. It therefore appears that the zebrafish does not process color information through chromatic opponent channels characteristic of vertebrate color vision. However, problems with the use of HFP to determine the spectral sensitivity function of the luminance channel are addressed. Finally, at the highest temporal rates, it appears that the ultraviolet sensitive cone type processes visual information faster than the middle and long wavelength sensitive cone types. It appears that temporal response rates of the cone types do not determine their relative contribution to separation of processing. This conclusion is supported only if the shortcomings of HFP cited in text are unfounded.

## **Chapter 1**

### Introduction

Patterns of light reflecting off objects in the environment allow visual creatures to see shapes, forms, light and dark, and color. There is anatomical evidence which demonstrates that the primate visual system processes color separately from luminance through parallel pathways or channels to the brain. Research also has demonstrated that the luminance (or broad-band) channel responds to transient or rapidly moving stimuli while the chromatic channel responds more to sustained or slowly moving stimuli. The visual signal begins at the photoreceptors in the retina which convert light energy into neural energy. There are two types of photoreceptors in the primate retina, rods and cones, which relay all visual signals to the other neurons of the retina. In humans, who possess three cone types, it is hypothesized that only cone types with high temporal resolution contribute to the luminance channel while cone types with slower temporal capabilities as well as those with high temporal resolution contribute to the chromatic channel.

While primates, including humans, appear to possess separate pathways which send chromatic and luminance information to different parts of the brain, lower vertebrates, such as teleost fish including zebrafish and goldfish, do not send visual information to the brain via anatomically separate pathways. However, previous researchers studying goldfish have demonstrated that their visual system can distinguish

between chromatic and luminance processing. Based on work with humans, primates, and goldfish, it appears that separate processing of chromatic and luminance information is common across many species and perhaps, fundamental to vertebrate vision even in the absence of anatomically separate pathways.

The zebrafish has recently become an important model for geneticists, developmental biologists, and vision scientists. To date, little research has been done on the physiological aspects of the zebrafish visual system and the relationship of their four cone types, including an ultraviolet sensitive cone, to separate visual processing. One technique that can be used to determine the cone inputs to the separate visual channels based on their different temporal properties is heterochromatic flicker photometry (HFP). In this project, HFP was used to determine the cone inputs of these channels in the zebrafish by recording the electrical activity of the retina. This project tested the hypothesis that the temporal properties of the cone types determine their contribution to the separate functional channels.

In addition, the temporal resolution of the four cone types in zebrafish was investigated. Based on the temporal responses of the four cone types, it was predicted that the spectral sensitivity of the luminance channel would correspond to the summation of the cones having high temporal resolution and that cones with slower temporal response rates as well as those with high temporal response rates would contribute to that of the chromatic channel.

To determine the cone inputs to the two channels, spectral sensitivities will be derived using HFP under temporal conditions known to isolate the responses of the



separate channels in goldfish. Low temporal flicker frequencies will be used to isolate the chromatic channel and high temporal flicker frequencies will be used to assess the luminance channel. A quantitative analysis of the contributions of each of the four cone types responsible for the separate responses of the low temporal frequency chromatic channel and the high temporal frequency luminance channel will be performed. The role of the temporal resolution of the different cone types in separate processing will be assessed. In addition, the contributions of a ultraviolet sensitive cone type to visual processing will be examined. The contributions of the three cone types to separate processing in humans is well known; however, the contribution of a fourth ultraviolet cone type to visual processing is relatively unknown. Based on the responses of the ultraviolet cone type, it will be determined whether the information provided by this cone type is useful to enhance the ability of zebrafish to sense luminance. This information will provide evidence regarding the role of ultraviolet vision in the natural environment of the zebrafish as well as other species that possess ultraviolet sensitive cone types.

## **Chapter 2**

### **Review of the Literature**

#### Overview

The purpose of the present project is to examine the role of separate processing of visual information in lower vertebrates. Separate processing of color and luminance in the visual system may be a fundamental component of all vertebrate vision. However, while many higher vertebrates have separate anatomical pathways from the eye to the brain, many lower vertebrates do not. Research will be presented that will demonstrate that some lower vertebrates do exhibit separate visual processing, in spite of the fact that there does not appear to be an anatomical separation of chromatic and luminance pathways. The purpose of this thesis was to determine the ability of the zebrafish, a lower vertebrate model, to exhibit separate visual processing of color and luminance. In addition, the temporal properties of the zebrafish cone types were determined to assess their role in contributing separately to the chromatic and luminance channels. The present review is divided into sections first discussing the optics, anatomy, and physiology of the eye. After discussing the eye, a review of the requirements of the visual system to process color and the theories of color vision including trichromatic theory and opponent process theory will follow. The review will continue with research on the anatomical and functional mechanisms of separate processing and how

heterochromatic flicker photometry can be used to examine the separate channels.

Finally, a summary of research on the zebrafish visual system will be given.

### Optics of the Eye

Light is absorbed, reflected, or refracted by the objects that it strikes in the environment. In order to follow the transmission of light information from the eye to the brain, it is important to understand the structure and function of the mechanisms through which vision occurs. Light enters the eye, first passing through the cornea. In non-aquatic animals, the cornea plays an important role in focusing most of the light entering the eye (Sekuler & Blake, 1994). The refractive power of the cornea is a result of the change in medium between air in the environment and the cornea. In aquatic animals, because there is little difference between water in the environment and the makeup of the cornea, its refractive power is limited (Powers & Easter, 1983). Aquatic animals have, therefore, developed a more powerful lens to compensate for the low refractive power of the cornea (Boynton, 1979). In addition, aquatic animals have developed a spherical lens which moves forward and backwards in the socket of the eye to focus on objects in the environment (Powers & Easter, 1983); this type of lens differs from the lens of non-aquatic animals which focuses images by being changed in shape.

### Anatomy and Physiology of the Eye

The environment provides such a vast amount of information that the visual system must filter the information at several levels. In order to accomplish this task, the visual system must organize and reduce the visual input. The electrical signals representing light stimuli pass through a series of organizing connections between

neurons. In the back of the eye is the retina, an extension of the central nervous system. The retina is formed by several layers of neurons and the synaptic connections between those neurons. The first layer of neurons in the retina is the photoreceptor layer. The somas or cell bodies of the photoreceptors are located in an area known as the outer nuclear layer. Their axons terminate in the outer plexiform layer where they synapse with bipolar, horizontal, and amacrine cells. The cell bodies of the horizontal, bipolar, and amacrine cells are located in the inner nuclear layer. Between the inner nuclear layer and the cell bodies of the ganglion cells is the inner plexiform layer; this layer contains the synapses between the bipolar and ganglion cells. Finally, the ganglion cells, the axons of which form the optic nerve, represent the last layer of neurons in the retina (Boynton, 1979).

Photoreceptors. Light passes through all of the layers of the retina before it strikes the photoreceptors. In most vertebrates, there are two kinds of photoreceptors known as rods and the cones. In the outer segments of the photoreceptors are chemicals called photopigments. When light strikes a photopigment molecule, the molecule undergoes a chemical transformation which causes an electrical change in the photoreceptor (Levine & Shefner, 1991). Once light is converted to neural energy by the photoreceptors, all information about the wavelength of the light that caused the chemical change is lost to the cell. Naka and Rushton (cited in Levine & Shefner, 1981) called this phenomenon the principle of univariance. The principle of univariance states that a photoreceptor can only change its rate of response once light energy is converted to

electrical energy (Sekuler & Blake, 1994). Subsequent neurons receive only changes in electrical responses from the photoreceptors rather than direct information from light.

All photopigments are differentially sensitive to different wavelengths of light. For example, rhodopsin, the photopigment contained in the rods of mammals, is maximally sensitive to 505 nm light and is less sensitive to other wavelengths of light (Levine & Shefner, 1981). In humans, there are three types of cones based on the photopigments which they contain in their outer segments. Each cone type is maximally sensitive to different wavelengths of light. In humans, the three cone types are maximally sensitive to light of 419 nm (short-wavelength cones), 531 nm (middle-wavelength cones), and 559 nm (long-wavelength cones) (Sekuler & Blake, 1994). Each of the three cone types is responsive to a range of wavelengths, but responds less to the other wavelengths of light to which they are sensitive. The spectral sensitivity function represents the sensitivity of the visual system to wavelengths of light in the visible spectrum. It depicts the combination of response inputs from the cones to different wavelengths of light.

Horizontal cells. Horizontal cells connect laterally to photoreceptors in the retina. Because of the wide interconnections of the horizontal cells, they respond to light over a wide area of the retina. Their response can be either excitatory or inhibitory depending on the nature of the stimuli that the photoreceptors signal to the horizontal cells (Levine & Shefner, 1991). Horizontal cells connect primarily to photoreceptors. A single photoreceptor may contact several horizontal cells thereby increasing the field of influence or receptive field of the photoreceptor. A receptive field is a conglomeration of

neurons that work together to form an area on the retina that signals a change in the pattern of light falling on the retina. Receptive fields allow the visual system to detect edges, changes in chromatic patterns, and differences between light and dark (Sekuler & Blake, 1994). Receptive fields also provide the mechanism by which the visual system exhibits chromatic opponency. More about receptive fields will follow in the discussion about bipolar cells.

Bipolar cells. Responses of the bipolar cells can be either excitatory or inhibitory depending on the location of the stimulation on its receptive field. The receptive fields of most bipolar cells are arranged in an antagonistic center/surround organization. Thus, light falling on the excitatory center of a receptive field causes an increase in response of the neuron. However, light falling on the antagonistic surround area causes an inhibition of the response. The bipolar cells are the first retinal neurons to exhibit a true center/surround receptive field organization.

Amacrine cells. Amacrine cells are responsive to transient stimulation and are probably responsible for the coding of temporal information in the retina. The ability of amacrine cells to signal temporal information is dependent on the information provided by previous cells, especially the photoreceptors where the visual signal originated. Amacrine cells respond most during stimulus onset and stimulus termination but respond little during sustained stimulation (Levine & Shefner, 1991). Amacrine cells form large receptive fields due to large lateral connections between bipolar cells similar to the connections made by horizontal cells.

Ganglion cells. Ganglion cells represent the final stage of processing in the retina. Axons from the ganglion cells form the optic nerve which transfers information from the retina to the brain. Hartline (1938) found three types of ganglion cells in frogs based on their response to white light and termed the three types on-cells, off-cells, and on/off cells. At the onset of a white light stimulus, on-cells responded rapidly with excitation for a brief time. Off-cells responded strongly with excitation when the white light stimulus was removed or turned off, and on/off cells responded highly with excitation at the onset and at the termination of the white light stimulus. Based on this work, it is apparent that different ganglion cells are designed to perform different tasks.

Kuffler (1953) was the first to determine that retinal ganglion cell receptive fields are arranged in a center/surround relationship. Studying the ganglion cells in cats, he found that a spot of light presented to the center of a receptive field caused either excitation or inhibition while light in the periphery of the receptive field caused the opposite response. Ganglion cells in the retinas of animals able to process color information are classified as spectrally opponent based on their responses. Receptive fields of spectrally opponent cells are arranged in a center-surround formation and respond differentially to lights of different wavelengths. For example, an excitatory long-wavelength cell increases the rate of response of the cell in the presence of long-wavelength light, while it decreases its rate of response to the presence of middle-wavelength light due to an inhibitory middle-wavelength cone input. Cells that cannot process color information are classified as spectrally nonopponent. Spectrally nonopponent cells increase their rate of response in the presence of any wavelength of

light to which they are sensitive. Thus, spectrally nonopponent cells respond to all wavelengths of light to which they are sensitive in a similar fashion.

Spectrally opponent ganglion cells are sensitive to differences in wavelength and provide the mechanisms necessary for the visual system to detect color. In general, these cells have smaller receptive fields so they are more sensitive to detail. Spectrally opponent cells also are designed for sustained responses (i.e., they respond best to slow stimuli) and do not respond well to fast transient stimuli (Kalat, 1992). Spectrally nonopponent cells, however, provide no color information to the visual system. Instead, they are designed to signal differences in luminance. To be maximally effective at signaling luminance changes across the retina, the spectrally nonopponent ganglion cells must receive information from a large number of preceding cells. Receiving information from a larger number of cells enhances the ability of the visual system to detect intensity changes but results in a reduced ability to represent detailed information. Also, spectrally nonopponent cells respond to fast transient stimuli that are not restricted to detail (Lee, Martin, & Valberg, 1988; Sekuler & Blake, 1994). In addition to being functionally separate, these types of cells are anatomically separate as well. Livingstone and Hubel (1988) report that nonopponent cells are larger and have larger receptive fields than spectrally opponent cells and each cell type transmits its signals to anatomically separate layers of the lateral geniculate nucleus (LGN).

### Requirements for Color Vision

Before discussing the theories of color vision, it is important to describe the requirements of any visual system to signal chromatic information. The first requirement



is that a visual system must have at least two photopigments with different but overlapping spectral sensitivities (Levine & Shefner, 1991). A monochromat (i.e., a subject with only one type of photoreceptor) can be shown any two wavelengths of light which, when adjusted properly in intensity, will be indistinguishable to that subject. Specifically, for a monochromat, any wavelength of light to which the photoreceptor type is sensitive can be adjusted in intensity so that it will affect the photoreceptor type in an identical manner as another wavelength of light. Recall that, according to the principle of univariance, once a photon of light is absorbed by an individual neuron, all information about its wavelength is lost to that neuron. Thus, any two wavelengths affecting a photoreceptor type identically will cause identical rates of responding in the visual system, making chromatic discrimination impossible (Levine & Shefner, 1991).

A dichromat has two types of photoreceptors, each with a different but overlapping spectral sensitivity function. Simply having different spectral sensitivity functions does not allow a dichromat to discriminate wavelengths of light. If the spectral sensitivity functions of the two photoreceptor types of a dichromat did not overlap, the principle of univariance would apply separately for each type of photoreceptor, much like the case in a monochromat (Boynton, 1979). However, if the spectral sensitivity functions of the two photoreceptors overlap across some wavelengths, lights of wavelengths which fall within this range will affect the two photoreceptor types differently thereby causing the two receptors to send different signals to the brain. There is only one wavelength of light that will affect both photoreceptors identically. The

neutral point is the wavelength that will cause identical reactions in both cone types. No other wavelength of light can be adjusted to cause confusion as with the monochromat (Sekuler & Blake, 1994).

Most humans, as well as many other animals, are trichromats (i.e., they have three types of cones, each with different but overlapping spectral sensitivity functions). Having three cone types enhances the ability of the visual system to signal different wavelengths (Sekuler & Blake, 1994). Finally, for animals with tetrachromatic visual systems such as those with a ultraviolet cone (U-cone) type, similar conditions follow.

In addition to having two or more cone types with overlapping spectral sensitivity functions, another condition necessary for color vision to occur is an opponent process whereby the visual system has neurons that produce opposite responses (i.e., inhibition or excitation) based on the wavelengths of light striking them. In humans, there appears to be an opponent process between signals from long and middle wavelength neurons and between short and the summation of long and middle wavelength neurons. More information about opponent processing in the visual system will be described in the discussion of the opponent process theory of color vision. Two theories have been proposed to account for color vision. The trichromatic theory was the first to be accepted. As a response to evidence unaccounted for by the trichromatic theory, the opponent process theory was proposed.

### Theories of Color Vision

Trichromatic theory of color vision. In 1672, Isaac Newton demonstrated that white light from the sun could be separated into the visible spectrum by passing it

through a prism (Hergenhahn, 1992). Newton proposed that white light is not a pure form of light, but rather is a mixture of all wavelengths of light in the visible spectrum. With further work, Newton found that white light could be formed from the mixture of three principle colors: red, blue, and green (Gregory, 1981). Applying Newton's observations, Thomas Young, in 1807, proposed the initial version of the modern trichromatic theory of color vision. Young's theory was modified by Herman von Helmholtz to become the trichromatic or Young-Helmholtz theory of color vision (Kalat, 1992). Young, and later Helmholtz, suggested that the combination of responses of three receptor types (red, green, and blue) was sufficient to allow the visual system to signal all colors. Trichromatic theory suggests that the relative rates of response of the three receptor types are translated into color information by the brain. In the 1960's, physiological evidence was found supporting the trichromatic theory. Through a process known as microspectrophotometry (MSP), researchers were able to investigate the photopigments of an excised eye. By subjecting the photopigments in the retina to lights of different wavelengths, researchers determined the rate of absorption of wavelengths by the individual photopigments. More recent confirmation of the presence of three cone types was provided by Dartnall, Bowmaker, and Mollon (cited in Zrenner et al., 1990). Using MSP techniques, Dartnall et al. confirmed that there are three cone photopigments in the human eye. Short-wavelength cones are most sensitive to light of 419 nm. Middle-wavelength cones are maximally sensitive to light of 531 nm and long-wavelength cones are most sensitive to light of 559 nm.

Opponent process theory of color vision. Opposing the view held by Young and Helmholtz, Ewald Hering proposed that color vision is a result of antagonism between opponent chromatic pairs (cited in Zrenner et al., 1990). Trichromatic theory argues that the color yellow is made possible through a combination of responses by long- and middle-wavelength cones. However, Hering argued that yellow is a basic color. Experiences such as chromatic afterimages are contrary to trichromatic theory, but support the opponent-process theory. When a field of one color (e.g., red) is presented to the visual system, human subjects report the presence of a green afterimage once the red field is removed. Chromatic afterimages are always in the color “opposing” the original stimulus (Hurvich & Jameson, 1957). Finally evidence suggesting that color blindness usually occurs in pairs (i.e., red vs. green or blue vs. yellow) lends further observational support to an opponent process theory of color vision (Levine & Shefner, 1991) as well as the fact that color combinations of “reddish-green” or “greenish-red” are contrary to normal chromatic experience (Zrenner et al., 1990).

Opponent process theory suggests that there are three opponent pairs that allow the visual system to signal color and luminance: red (L-cones) versus green (M-cones), blue (S-cones) versus yellow (M-cones plus L-cones) , and black versus white (Zrenner et al., 1990). The first psychophysical evidence in support of the opponent process theory of color vision was presented by Hurvich and Jameson (1957). Using a process known as hue cancellation, Hurvich and Jameson determined the antagonistic spectral sensitivity distribution of the human visual system. In the process of hue cancellation, a subject is shown a particular wavelength (e.g., corresponding to blue). Other lights of wavelengths

corresponding to yellow are also presented. Subjects were asked to compare the mixture of the two stimuli and report which combination looked neither blue nor yellow. Hurvich and Jameson demonstrated that the energies of the two wavelengths necessary to cancel the effects of the yellow-blue (and red-green for other stimuli) antagonistic response corresponded to opponent process pairs.

The first physiological evidence supporting the opponent process theory of color vision was provided by DeValois, Abramov, and Jacobs (1966). Recording electrical responses from single cells in the LGN of the macaque monkey, they presented flashes of different wavelengths of light equated for luminance. They found three types of neurons which exhibited different types of responses. A neuron could either increase its response rate relative to its spontaneous rate (rate of response in the absence of stimuli), decrease its relative response rate, or increase its rate of response to some wavelengths and decrease its response rate to other wavelengths. Cells that responded only with an increase and cells that responded only with a decrease were called spectrally nonopponent cells because they did not change their type of response across wavelengths of light. Cells that increased responding to some wavelengths and decreased responding to other wavelengths were termed spectrally opponent cells. DeValois et al. further classified the spectrally opponent cells based on the wavelengths of light to which they responded. One type of cell was excitatory to long wavelengths and inhibitory to middle wavelengths (+red vs. -green); another group of cells responded in the opposite manner to middle and long wavelengths (-red vs. +green). Two other groups of cells were classified in a similar manner. One group increased responding to short wavelengths and decreased their rate of

responding to the summation of long and middle wavelengths (+blue vs. -yellow).

Another group responded in the opposite manner (-blue vs. +yellow).

Based on these findings, it appears that both the trichromatic theory and the opponent process theory are correct. Using MSP, researchers found that all light information utilized by the human visual system including chromatic, temporal, and intensity information is first encoded by three cone types maximally sensitive to short, middle, and long wavelengths of light. However, evidence supporting opponent process theory suggests that antagonistic responses between cells responsive to pairs of wavelengths is necessary at higher levels in the visual system.

#### Anatomical Separation of Visual Processing Pathways

Research on the response patterns of the LGN neurons in macaques (DeValois, Abramov & Jacobs, 1966; Schiller & Malpelli, 1978) and on retinal ganglion cells in primates (Kremers, Lee, & Kaiser, 1992; Lee, Pokorny, Smith, Martin, & Valberg, 1990; Schiller & Logothetis, 1990; Schiller & Malpelli, 1978 ) and cats (Enroth-Cugell & Robson, 1966; Hochstein & Shapley, 1975) suggests that higher vertebrates process visual information via separate anatomical pathways or channels.

One of the original studies that demonstrated that visual information is processed by anatomically separate pathways was with cat ganglion cells. Enroth-Cugell and Robson (1966) found that cat ganglion cells could be cast into one of two groups, as either X-cells or Y-cells, based on their spatial summation of the signals across their receptive field. The spatial summation of X-cells is linearly related to receptive field illumination. Unlike X-cells, Y-cells do not exhibit linear summation based on the

illumination of the photoreceptors. Enroth-Cugell and Robson (1966) also measured the size of the retinal receptive fields of both X-cells and Y-cells and found that the receptive fields of Y-cells were larger than the receptive fields of X-cells. Sherman and Spear (cited in Kalat, 1992) found that there is an anatomical distinction between X-cells and Y-cells based on cell size such that X-cells are physically smaller than Y-cells. In addition to anatomical separation, Enroth-Cugell and Robson (1966) found that X-cells are able to respond to more finely detailed stimuli than Y-cells based on the sizes of the receptive fields. Hochstein and Shapley (1976), recording from the retinal ganglion cells in cats, confirmed the results of Enroth-Cugell and Robson (1966). Further distinction between X-cells and Y-cells was provided by Stone and Freeman (cited in Levine & Shefner, 1991) who found that the axons of Y-cells conduct signals faster than X-cells. They also found that Y-cells respond to fast moving stimuli while X-cells respond to slow or nonmoving stimuli. A similar distinction has been found in lower vertebrates including the goldfish. Bilotta and Abramov (1989) classified goldfish retinal ganglion cells as X-like or Y-like based on their spatial summation properties.

A similar anatomical distinction between types of processing in neurons has been made in higher vertebrates including humans and nonhuman primates. Livingstone and Hubel (1988) state that, in humans, the axons from ganglion cells which form the optic nerve split to transfer information to the LGN and the superior colliculi. The LGN of primates is comprised of six distinct layers of cells separated by axons. The two innermost layers are called magnocellular layers because the cells forming those layers are large (magno, meaning large). The four outermost layers are known as parvocellular

layers because the cells forming these layers are smaller (parvo, meaning small).

Livingstone and Hubel further suggest that about 90% of parvocellular ganglion cells (P-cells) transmit color-opponent information to the LGN while the magnocellular ganglion cells (M-cells) do not transmit color information. Studying the functional aspects of the parallel pathways in humans, Livingstone and Hubel found that the M-pathway transmits signals to the LGN more rapidly than does the P-pathway. They also found that the M-pathway is more sensitive to low contrast stimuli.

There are several physiological differences between M- and P- pathways in primates. Magnocellular layers of the LGN and M-cells in the retina do not receive color-opponent signals while most of the parvocellular layers in the LGN and P-cells in the retina respond to particular wavelengths of light in a color-opponent fashion. Recording from the LGN of macaques, Schiller and Malpelli (1978) determined that most parvocellular neurons in the LGN were color opponent and that the magnocellular layers responded in a broad-band fashion to most wavelengths (i.e., there was no color opponency). Schiller and Malpelli further found differentiation between magnocellular and parvocellular layers of the LGN based on their temporal properties. By comparing the number of action potentials during the first 75 ms after stimulus onset and the number of action potentials in a 75 ms period 140 ms following stimulus onset, they found that parvocellular layers respond in a sustained manner while magnocellular layers respond in a rapid, transient manner. They also found that the axons projecting from the retina to the LGN conduct their signals in a similar temporal relationship. M-cell axons conduct their signals very rapidly, while P-cells transmit signals more slowly. They found no cells that



responded counter to these indications suggesting that there is a clear separation of the pathways from M-cells and P-cells in the retina to magnocellular and parvocellular layers in the LGN based on their temporal responses.

Schiller and Logothetis (1990) investigated the effects of selective lesioning in the LGN of macaques. They found that M and P connections carry out processing concurrently and have separate and specific functions. They first determined that about 90% of ganglion cells are color-opponent and project to the parvocellular layers of the LGN. The remaining 10% are responsible for magnocellular inputs. They also determined that the rods, when active, function through the magnocellular layers of the LGN. By selectively lesioning the parvocellular layers of macaque LGN, Schiller and Logothetis found behavioral deficits in color discrimination, form and pattern recognition, and stereopsis. By lesioning the magnocellular layers of the macaque LGN, they found behavioral deficits in the perception of movement and the perception of flicker. Schiller and Logothetis suggest that these results demonstrate the different functions provided by the two parallel pathways.

These differences in function, according to Livingstone and Hubel (1988), are a result of evolutionary developments. They propose that the magnocellular system is more primitive than the parvocellular system. The magnocellular system performs essential visual functions that are necessary for survival including detecting the movements of predators or prey. The two systems allow for different types of functioning. The magnocellular system is responsible for perception of fast stimuli and allows for fast decisions. The parvocellular system allows for non-necessary functions to

be performed at a slower speed including the perception of color. Furthermore, the separation of functions, according to Livingstone and Hubel, isolates damage and allows the different pathways to process different aspects of stimuli simultaneously, thereby increasing the overall speed of processing.

This research has demonstrated that most vertebrates process visual information through separate pathways. The original distinction between separate mechanisms of visual processing was made between X-cells and Y-cells in the cat retina (Enroth-Cugell & Robson, 1966). Other research has demonstrated that these cells differ in receptive field size, their ability to detect detailed stimuli (Enroth-Cugell & Robson) and their rate of conduction through their axons (Hochstein & Shapley, 1976).

Many researchers (Livingstone & Hubel, 1988; Schiller & Logothetis, 1990; Schiller & Malpelli, 1978) discovered similar pathways in primates which differ in the anatomical and functional mechanisms through which they transmit visual information. Magnocellular pathways are responsible for signaling changes in luminance and movement. They respond in a rapid, transient manner to stimuli and transmit their signals very rapidly to the LGN. Parvocellular pathways signal color information and detailed stimuli. They respond in a sustained or slow manner and conduct signals to the LGN at a slower speed than the magnocellular pathways.

In species which display anatomical and functional separation of visual processing, there are two common characteristics. In X- and Y-cells in cats as well as M- and P-cells in primates, there is a distinction between the types of temporal stimuli that can be transmitted by each mechanism. Both Y- and M-cell types conduct their

transmissions rapidly and respond to transient stimuli. In addition, both X- and P-cell types conduct their signals slowly and respond to sustained stimuli. Also, X- and P-cells have small receptive fields, and as a result, are responsible for the transmission of information about detailed stimuli. Conversely, Y- and M-cells have larger receptive fields and signal changes in luminance.

While teleost fish such as the goldfish do not process visual information at the LGN like higher vertebrates, previous researchers have demonstrated a distinction between mechanisms of visual processing. Mackintosh, Bilotta, and Abramov (1987) classified ganglion cells in the retina of goldfish as either spectrally opponent or spectrally nonopponent based on their response to chromatic stimuli. Neumeyer, Wietsma, and Spekreijse (1991) demonstrated behaviorally that goldfish process chromatic and luminance information separately. In this study, goldfish were trained to respond to a dark field or an illuminated field to test their discrimination of luminance and color respectively. At low levels of adaptation, animals trained to the illuminated field could discriminate based on their processing of luminance information but not color information. These findings suggest that mechanisms may exist in lower vertebrates to process visual information separately depending on stimulus parameters. Gouras and Zrenner (1979) have demonstrated that some opponent ganglion cells in the macaque monkey show a summated response to high rates of flicker characteristic of the luminance channel. They explain this finding by suggesting that the opponent cells undergo a frequency dependent phase shift between the center and surround mechanisms at high temporal frequencies--that is, the latency of response from the surround is greater

than the latency of response from the center mechanism. At low flicker frequencies, responses of the center and surround mechanisms are out-of-phase, and thus antagonistic, resulting in color opponency. At higher flicker frequencies, the latencies of responses from the center and surround mechanisms become decreasingly out-of-phase and begin to summate.

Similar patterns of response have been found in the goldfish (Bilotta & Abramov, 1989). Some Y-like cells in the goldfish responded like X-like cells at low spatial frequencies and like Y-like cells at higher spatial frequencies. Similarly, as found in primate ganglion cells by Gouras and Zrenner (1979), the center and surround antagonism characteristic of goldfish X-like and Y-like cells summates at high temporal frequencies. In addition, research on goldfish by Mackintosh, Bilotta, and Abramov (1987) has shown that ganglion cells that respond in a nonopponent manner show opponency when the threshold to long- and middle-wavelength cones are increased by chromatic adaptation. This research suggests that anatomical separation is not necessary for the visual system to process different aspects of the visual environment differently. Rather, color opponent ganglion cells can respond with opponency at low flicker frequencies and with summation at higher flicker frequencies thereby processing stimuli differently based on temporal factors.

The distinction between these visual mechanisms may be driven by the temporal properties of the cone types which provide inputs to the separate visual channels. Research by Gouras and Zrenner (1979) and Bilotta and Abramov (1989) demonstrates the importance of temporal factors in the different types of responses of individual cells.

In primates, the temporal responses of the short-wavelength cones are not as rapid as that of the middle- and long-wavelength cones. Therefore, short-wavelength cones can contribute to the chromatic channel but cannot respond in a rapid manner to high frequency stimuli characteristic of luminance channel processing (Boynton, 1979). It is possible that the temporal resolution of the cone types themselves determines which types of cones contribute to the separate visual channels.

#### Using HFP to Determine the Cone Inputs to Separate Channels

As previously described, color opponent cells respond in a sustained manner to stimuli while spectrally nonopponent cells respond transiently to stimuli. Using a technique called heterochromatic flicker photometry (HFP), researchers can isolate the functioning of both the color-opponent and luminance channels based on their temporal characteristics. This method requires that lights of two different wavelengths (or a white light and a monochromatic light) be presented out-of-phase of one another. This type of stimulus presentation produces the perception of flicker in humans and presumably animals (Eisner & MacLeod, 1980; Regan, Schellart, Spekreijse, & van den Berg, 1975). When the intensities of the two lights are adjusted so that each stimulus has the same effectiveness on the visual channel, the perception of flicker is minimized. This isoluminant value can be used to examine the sensitivity of the channel to various wavelengths of light. The inverse of that stimulus intensity is the sensitivity of the visual system to the test wavelength (Eisner & MacLeod, 1980; Regan et al., 1975).

By varying the stimulus parameters, one can isolate either of the visual channels and determine its spectral sensitivity function. For example, to isolate the opponent color

channel, flickering lights of different wavelengths at a low temporal frequency would be used to stimulate the response of the spectrally opponent cells or chromatic channel. Similarly, to isolate the luminance channel, two wavelengths of light would be flickered at a high temporal frequency which stimulates only spectrally nonopponent mechanisms (King-Smith & Carden, 1976; Lee, Martin, & Valberg, 1988; Loop, Millican, & Thomas, 1987). By adjusting the rate of flicker, either channel can be isolated. The spectral sensitivity of both the luminance and the opponent color channels can be determined by using both high and low temporal rates of flicker across wavelengths.

The advantage of using HFP to derive spectral sensitivity functions for the separate channels is that both psychophysical and physiological measures can be used to find the isoluminant points of various stimuli. HFP has been used with psychophysical methods to derive the goldfish spectral sensitivity function based on isoluminant points (Bilotta et al., 1994). HFP also can be used to examine the visual effectiveness of stimuli from electroretinogram (ERG) responses. The ERG is a gross recording measure of the electrical activity of the retina. The resulting ERG response has distinguishing components which allow researchers to identify the functioning of the individual neural layers of the retina. When a visual stimulus is first presented to the eye, the ERG shows an initial decrease in voltage corresponding to the activation of the photoreceptors (the a-wave) (Hanitzsch, Lichtenberger, & Mattig, 1996). The ERG b-wave follows the a-wave and is recognized by a sharp positive increase in response voltage corresponding to the functioning of the bipolar cells (Brown & Wiesel, cited in DeMarco & Powers, 1991). The c-wave is believed to represent noise or other processing in the eye. The d-wave

corresponds stimulus termination and is recognized by a sharp positive increase in electrical potential. Regan et al. (1975) measured the effect of flickering chromatic stimuli on the goldfish ERG. Using HFP procedures, they alternated presentations of a monochromatic light of various intensities with a white light. The intensity of the monochromatic light where the amplitude of the ERG b-wave was minimized was defined as the isoluminant point. They determined the spectral sensitivity of the goldfish visual system by plotting these sensitivities to different wavelengths of light across the spectrum. Regan et al. further found that the spectral sensitivity function determined by HFP was relatively stable across different stimulus backgrounds.

### Zebrafish Model

The zebrafish (*Danio rerio*) has recently become an important model for neuroscience research. Its ability to propagate rapidly and prolifically is of special interest to geneticists. Genetic discoveries have led to an increase in interest of researchers in many fields including developmental biology and vision research (Barinaga, 1990). Of further interest to vision researchers is the discovery that zebrafish appear to possess four cone types, including one that is sensitive to ultraviolet wavelengths of light (Robinson, Schmitt, & Dowling, 1995). There is conflicting research, however, concerning the presence of ultraviolet sensitive cones (U-cones) in the zebrafish retina. Nawrocki et al. (1985) suggest that, although the zebrafish has four cone types, there are only three types of photopigments in the zebrafish retina. Using MSP techniques on adult zebrafish, they determined that fish tested 6-8 days post-fertilization had four photopigments (i.e., three cone photopigments and one rod photopigment).

Clark (1981) reports the presence of four anatomical cone types with absorbance maxima of three of the cone types at 417 nm, 485 nm, and 558 nm. More recent evidence from Robinson, Schmitt, and Dowling (1995) has demonstrated that U-cones are the first to develop followed by the short, middle, and long wavelength sensitive cones. Other research by Robinson, Schmitt, Harosi, Reece, and Dowling (1993) using MSP found that there are four cone photopigments in zebrafish which are maximally sensitive to long (570 nm), middle (480 nm), short (415 nm), and U (362 nm) wavelengths of light and that each of the four cone types are quite prevalent in the adult zebrafish retina. They report that 25% of the cones in the retina of adult zebrafish are sensitive in the ultraviolet range.

The zebrafish provides an interesting opportunity to study the role of U-cones in an adult teleost fish. Research on other teleost fish including the Atlantic salmon (Kunz, Wildenburg, Goodrich, & Callaghan, 1994) and the rainbow trout (Browman & Hawryshyn, 1994) suggests that both types of fish lose their ultraviolet sensitivity as they become adults. This loss in sensitivity has been attributed to normal cell death (Kunz et al., 1994). Robinson, Schmitt, and Dowling (1995) have determined that the zebrafish possesses the U-cones into adulthood. Past research on the zebrafish visual system has attempted to identify the anatomical structures of its retina. However, research on retinal processing and the separation of visual processing in the zebrafish is lacking. Also, there has been little research on the role of U-cones in separate processing of visual information including chromatic and luminance processing. Previous research on the separation of visual processing has focussed especially on primates with trichromatic



visual systems (Livingstone & Hubel, 1988; Schiller & Logothetis, 1990; Schiller & Malpelli, 1978). The role of four cone types in separate visual processing has not been addressed by previous research. It is unknown how the addition of a fourth cone type will affect the dispersion of cone inputs to the separate channels.

### Summary

This review demonstrates that parallel processing is present in many species that possess anatomical separation of pathways to the LGN. The review also provided brief evidence suggesting that separate processing may occur in species such as teleost fish without anatomically separate pathways. These findings lead to the question of whether parallel processing is a fundamental property of vertebrate vision. This review further prompts the question of which cone types contribute to the chromatic and luminance channels. Previous literature has not conclusively addressed either of these questions, especially in species with four cone types. Therefore, the purpose of this thesis project is to

1. Determine whether zebrafish process visual stimuli in a separate manner. It is hypothesized that they will exhibit separate processing of chromatic and luminance information. It is hypothesized that separation of visual processing is a fundamental component of the vertebrate visual system. Previous research on a wide number of higher vertebrate models has demonstrated some form of separate visual processing.

2. Determine the temporal resolution of each of the four cone types in the zebrafish. It is hypothesized that those cone types with high temporal resolution will provide inputs to the chromatic and luminance channels while those cone types with low

temporal resolution will only provide inputs to the chromatic channel. The luminance channel transmits visual signals very rapidly. Rapid processing at the photoreceptors seems to be a necessary requirement for subsequent neurons to transmit visual signals very rapidly. The chromatic channel send signals more slowly so does not require cone inputs that have fast temporal resolution.

## Chapter 3

### Method

#### Participants

Adult zebrafish (*Danio rerio*) 4-5 cm in length were obtained from Scientific Fisheries (Huntington Beach, CA) and were maintained on a 14 hr light/10 hr dark cycle with about 20 fish housed per 10 gallons of water. Animals were fed daily with TetraMin Basic Flakes tropical fish food. Animals were handled in accordance with procedures approved on January 24, 1996 by the Institutional Animal Care and Use Committee at Western Kentucky University.

#### Apparatus

Electrophysiological apparatus. Animals were tested in a plexiglas tank measuring 3.8 cm high by 3.3 cm wide by 7.6 cm deep. An open window in the right side of the plexiglas tank measuring 3 cm by 2.3 cm allowed uninterrupted passage of light stimuli presented via a liquid light guide (Oriol, Stratford, CT, Model 77556). The plexiglas tank was located in a Faraday cage measuring 76.2 cm in height by 55.9 cm in width by 45.7 cm in depth. Electroretinograms (ERGs) were obtained using a 36 gauge chlorided silver electrode positioned intervitreally in the right eye of the subject via a micromanipulator (WPI, Sarasota, FL, Model MM-3). The experimenter used a stereomicroscope (Edmund Scientific, Barrington, NJ, Model D39,361) to position the electrode in the eye. A 36 gauge chlorided silver reference electrode was placed in the

nostril of the subject. Electrical signals from the eye passed through an AC differential amplifier (WPI, Sarasota, FL, DAM-50) with a bandpass of 0.1 to 100 Hz. The signal from the amplifier was sent simultaneously to a 60 MHz dual channel oscilloscope (Tektronix, Beaverton, OR, Model 2215A) and the data acquisition board (Scientific Solutions, Solon, OH, Lab Master DMA) of the laboratory computer (DTK, Chicago, IL, Tech-1663) where it was stored for later analyses. The sampling rate of the data acquisition board was 250 Hz.

Optical system. Light stimuli were generated by a two-channel Maxwellian view optical system. The background channel presented stimuli primarily in the visible spectrum (i.e., 400 nm to 750 nm) while the test channel provided stimuli in the ultraviolet and visible range (i.e. 320 nm to 750 nm). The light source for the test channel was a 150 W xenon arc lamp (Spectral Energy, Westwood, NJ, Model LH 150). Light from the arc source was collimated by a quartz lens measuring 54 mm in diameter (quartz glass allows transmission of ultraviolet and visible wavelengths of light). The collimated beam passed through quartz windows to a water bath measuring 105 mm in length. The water bath served as a heat filter by absorbing infrared wavelengths. Another quartz lens refocussed the light onto a shutter vane which was controlled by a stepper motor (Alpha Products, Fairfield, CT, Model ST-143) that was driven by the laboratory computer. Light was recollimated by a quartz lens before it passed through an interference filter measuring 50 mm in diameter. Interference filters with a half-bandwidth of 10 nm controlled stimulus wavelength. The peak transmission wavelengths of the interference filters were: 320, 340, 360, and 380 nm (Andover Corporation,

Andover, NH, Model FS10-50), and 400 nm through 700 nm in 20 nm steps (Oriel, Stratford, CT, Model 54161). After leaving the interference filters, light passed through a series of quartz neutral density filters (Reynard, Calle Sombra, CA, Model 398) which controlled stimulus intensity. The neutral density filters were placed in series to attenuate the light over a 6 log unit range. Attenuation was possible within 0.1 log unit steps. Each neutral density filter was 50 mm square. Light then passed through a polka-dot beam mixer (Oriel, Stratford, CT, Model 38106) measuring 51 mm square. Light was focused by a quartz lens in front of a liquid light guide (Oriel, Stratford, CT, Model 77556) measuring 5 mm in diameter by 1 m long which transmitted a diffuse stimulus to the eye.

The background beam source, which projected primarily visible wavelengths, was a 250 W tungsten/halogen bulb (Oriel, Stratford, CT, Model 6334) powered by a 24 V, 12 A, DC power supply (Condor, Oxnard, CA, Model F24-12-A+). Light passed through a KG-2 type heat filter (Rolyn Optics, Corina, CA, Model 65.3025), 50 mm square, which blocked the transmission of short ultraviolet and infrared wavelengths. The filament source was collimated by a lens, then refocused onto a shutter vane similar to that used in the test beam. Light was recollimated by a lens and passed through a series of neutral density filters similar in attenuation values to those used in the test beam. The collimated beam was reflected by a mirror to the polka-dot beam mixer in the test channel where it was mixed with the test beam and focused in front of the liquid light guide. All optical components were mounted on an optics breadboard (Aerotech, Pittsburgh, PA, Model V 2448). Light measurements were converted to quanta/cm<sup>2</sup>/s from values provided by a

radiometer (E.G. & G, San Diego, CA, Model 550-2) sensitive to ultraviolet and visible wavelengths. The Appendix lists the actual irradiance in quanta/cm<sup>2</sup>/s transmitted at each wavelength with no attenuation.

### Procedure

Each subject was anesthetized by immersion in a 0.04% solution of tricaine methanesulfonate and then paralyzed by an intramuscular injection of 4 µl of gallamine triethiodide. A hole was made in the sclera of the right eye of the subject with a 26 gauge syringe needle to allow the entry of the test electrode. Individual animals were placed in a pliable plastic holder which was positioned within a plexiglass holding tank with sponges. The eye of the subject remained above the water line. Subjects were artificially respired by a pump (Aquarium Systems, Mentor, OH, Model MN 404) which circulated an aerated solution of water and 0.01% tricaine methanesulfonate over the gills to continuously respire and anesthetize the subject. Water entered the plexiglas tank via a tube which was located 1.2 cm above the base of the tank. Excess water was drained from the opposite end of the plexiglas tank via a tube which was located 1.8 cm from the base of the tank. Following the experiment, the subject was sacrificed by cervical separation and disposed of according to standard procedures approved by the Institutional Animal Care and Use Committee of Western Kentucky University on January 24, 1996.

There were two separate testing procedures in the present study: the Heterochromatic Flicker Photometry (HFP) procedure and the Temporal Response (TR) procedure.

HFP procedure. Once the animal was placed in the recording chamber with the electrodes properly positioned, it was adapted to a white background light of 5.22  $\mu\text{W}/\text{cm}^2$  for at least 10 min. By adapting the animal to this intensity of white light, it ensured that the visual response was a result of the functioning of the cones and not the rods (Neumeyer et al., 1991). Following adaptation, the white light standard stimulus was flickered out-of-phase in a square wave presentation with lights of 320, 340, 360, 380, 400, 420, 440, 480, 520, 560, 600, and 640 nm for 4 s at either a high (16 Hz) or low (4.6 Hz) flicker rate. These wavelengths were chosen to represent critical points in the spectral sensitivity function of the zebrafish (see Figure 1). Initially, the standard light was flickered with either 320 nm light or 600 nm light. The presentation order of other wavelengths then progressed in numerical sequence, either ascending or descending depending on the starting wavelength (i.e., 320 nm or 600 nm) skipping every other wavelength until the maximum value (or minimum depending on the starting wavelength) was tested. Then the progression was reversed through the previously skipped wavelengths. This staggered progression was intended to minimize stimulus order effects and ensure that sufficient data across the entire range of wavelengths was collected on each fish. At each wavelength, all irradiance values were presented in order, beginning at -6.0 log units attenuation and increasing in 0.5 log unit steps. Using software written by the experimenter, ERG responses in the form of voltages were collected by the laboratory computer. To determine the isoluminant point, the experimenter assessed on-line the stimulus irradiance at which the ERG b-wave amplitude was minimized via a Fourier decomposition of the ERG response. The preliminary analysis was displayed on

the computer monitor so the experimenter could assess the irradiance at which the visual effectiveness of the test and background lights reversed. Each subject was presented with the test light at -6.0 log units attenuation. The irradiance of the test light was then increased in 0.5 log unit steps until the isoluminant or minimum response point was found. Irradiance was then further increased until a strong response was again attained due to the reversal of visual effectiveness of the test and background lights.

Temporal response procedure. Each subject was positioned in the subject holder and the electrode was lowered into position. Prior to stimulus presentation, a white adaptation light of  $5.22 \mu\text{W}/\text{cm}^2$  was presented for at least 10 min to ensure only cone responses. For all test sessions, the adaptation light remained on during the presentation of the test light. The temporal response of the long wavelength cone type ( $\lambda_{\text{max}} = 570 \text{ nm}$ ) was determined by flickering a 600 nm light at -2.0 log units attenuation for 4 s at the temporal frequencies of 1, 2, 4.6, 8, 16, 20, and 24 Hz. By using a long-wavelength light, the ERG b-wave component was comprised primarily of the response of the long-wavelength cones (see Figure 1). To determine the temporal response of the middle-wavelength cones ( $\lambda_{\text{max}} = 480 \text{ nm}$ ), a 600 nm light at -2.3 log units attenuation was presented for at least 10 min prior to testing to increase the response threshold of the long-wavelength cones. A 500 nm light at -2.0 log units attenuation was then flickered in the manner previously described. By chromatically adapting the long-wavelength cones, the ERG b-wave component at this wavelength was comprised primarily of the response of the middle-wavelength cones. Short-wavelength cones ( $\lambda_{\text{max}} = 415 \text{ nm}$ ) were tested in a similar manner by flickering a 420 nm light at -2.0 log units attenuation after



chromatically adapting the middle-wavelength cones to a 500 nm light at -2.0 log units attenuation. The temporal resolution of the U-cones ( $\lambda_{\text{max}} = 362 \text{ nm}$ ) was determined by flickering a 360 nm light at -0.5 log units attenuation after chromatically adapting the short wavelength cone to a 440 nm light at -0.3 log units attenuation. All background intensities (whether white or chromatic backgrounds) were set to approximately  $5.22 \mu\text{W}/\text{cm}^2$  to ensure that differences in intensity were not producing differences in responses across test conditions. This intensity is the same as that used during the HFP procedures.

## Chapter 4

### Results

#### ERG Signal Averaging

Prior to analysis, all ERG responses were subjected to a number of procedures to enhance the retinal signal and minimize electrical noise. First, ERG responses were subjected off-line to a moving average software filter (see Vennat, Besse, Sanzelle, Doly, & Gaillard, 1994) written by the experimenter. Since ERG signals originating in the eye are amplified by a factor of 10,000 before being collected by the laboratory computer, 60 Hz noise from the electrical currents supplying power to the building as well as electrical activity of the laboratory equipment also are collected by the test electrode and amplified. Since most of the noise is consistently located at 60 Hz, it can be filtered out leaving the ERG signal virtually preserved. This “notch” filter reduces 60 Hz input leaving frequencies except those very near to 60 Hz intact. Software filtering is a common noise reduction technique used in physiological investigations. Figure 2a and Figure 2b show unfiltered ERG responses of one subject to a 440 nm light at -2.0 log units attenuation to 4.6 Hz and 16 Hz HFP stimuli respectively. The unfiltered 4.6 Hz ERG peak responses in Figure 2a can be differentiated although the signal is not clear. In Figure 2b, the unfiltered 16 Hz ERG responses are difficult to discern from the 60 Hz noise. Figure 3a and Figure 3b show the ERG responses from Figure 2 after passing through the notch filter. It is apparent that the filter clarified the signal for both the 4.6 Hz and 16 Hz ERG responses. In Figure 3a, there are about 4.6 ERG responses per 1000

ms which can easily be counted. The 16 Hz ERGs in Figure 3b are not as clear since the timing of the ERG response is so rapid. For clarity, Figure 4 shows a 1000 ms segment of the 16 Hz ERG shown in Figure 3b. The 16 individual ERG responses are separated by dashed vertical lines. Many of the ERGs in Figure 4 show double peaks typical of 16 Hz ERG responses (see below).

After filtering, the ERG responses were averaged together across stimulus cycles. The purpose of averaging was to further enhance the response to noise ratio. With software written by the experimenter, averaging was accomplished by superimposing each ERG response during each stimulus cycle and then dividing the summated response by the number of ERG responses superimposed. Only ERG responses collected during the last 3000 ms were used in the averaging procedure because of the large initial response to stimulus initiation (see Figure 3a and Figure 3b). This initial response is typical in ERG recording (personal observation; see also Brockerhoff et al., 1995). After the first 1000 ms of stimulus flicker, the ERG responses become very steady as seen in Figure 3a and Figure 3b. Fourteen ERG responses to 4.6 Hz stimuli were averaged and forty-seven ERG responses to 16 Hz stimuli were averaged for each stimulus cycle. Figure 5a shows the averaged ERG response of the ERG train shown in Figure 3a. The initial rise in response amplitude is the b-wave of the ERG. Also note the second peak (second b-wave) after the initial b-wave. The arrow designates the time of stimulus change from the white light to the monochromatic test light. Figure 5b shows the averaged ERG response to the 16 Hz stimuli shown in Figure 3b. Note the double peaks present in the averaged ERG which were weak in the unaveraged 16 Hz ERG response

shown in Figure 4. The second peak is most likely the b-wave resulting from the second stimulus presentation. The arrow indicates the change of stimuli from the white background light to the monochromatic test stimulus.

After averaging, the ERG responses were subjected to a Fourier decomposition to assess the response amplitude to each stimulus condition. Preliminary analysis showed that most of the response amplitude to 4.6 Hz and 16 Hz stimuli was accounted for by the amplitude of the fundamental Fourier response component. Similar findings are reported by Regan et al. (1975). Using the amplitude of the fundamental Fourier response component provides a more quantitative measurement of the responses compared to extracting the maximum value from the ERG response.

#### Heterochromatic Flicker Photometry (HFP)

Spectral sensitivity functions. To investigate the first hypothesis that zebrafish process visual information separately, ERG responses were recorded at several irradiances for each of the 12 wavelengths flickering out-of-phase with a  $5.22 \mu\text{W}/\text{cm}^2$  white light at 4.6 and 16 Hz. Responses were collected from 12 zebrafish retinæ. Irradiance-response functions were determined for each fish at 4.6 and 16 Hz at each wavelength by plotting stimulus irradiance by the amplitude of the Fourier fundamental response component based on the ERG b-wave component. For most stimulus presentations, the ERG b-wave matched the frequency of the stimulus which had the greatest effectiveness on the retina--that is, one of the two stimuli (white or monochromatic light) stimulated the retina more than the other stimulus. As the irradiance of the monochromatic stimulus changed, so did the relative effectiveness of the

two stimuli. The isoluminant point was represented by the stimulus irradiance for a given wavelength where the ERG b-wave amplitude was minimized. It was at this point that the two stimuli were approximately equivalent in visual effectiveness. The isoluminant point was defined as the irradiance of the monochromatic light at which the amplitude of the ERG b-wave was minimized (see Regan et al., 1975). Figure 6 shows three ERG response trains to stimuli of 420 nm at irradiances of -2.5, -4.0, and -6.0 log units attenuation flickering out-of-phase with the white light (Figures 6a, b, and c, respectively). The retina responds more to the test light at -2.5 log units attenuation than to the white light resulting in the large ERG response amplitude (Figure 6a). Figure 6b shows the ERG response after the irradiance of the monochromatic test light has been reduced to -4.0 log units attenuation. No clear ERG response is discernable because the 420 nm test light and the white background light are approximately equal in generating visual responses in the retina. This point represents the isoluminant point for this test wavelength. As the irradiance of the monochromatic test light is further reduced to -6.0 log units attenuation, the white light causes a stronger retinal response resulting in an increase in ERG response amplitude to the white light as shown in Figure 6c. Figure 7 shows the irradiance-response function representing the ERG responses in Figure 6 as well as other irradiances. The isoluminant point selected from this figure is at -4.0 log units attenuation which is the lowest amplitude of the fundamental Fourier component. Figure 8 shows another irradiance-response function from the same subject to a different monochromatic test stimulus. The test stimulus consisted of a 520 nm light presented out-of-phase with a white light presented at a temporal rate of 16 Hz. Based on the

individual irradiance-response functions for each wavelength, isoluminant points were determined under both flicker frequencies. For irradiance-response functions for which there were more than one apparent minimum point (see Figure 9), the isoluminant point was defined as the irradiance at which the response was of the lowest amplitude and at which responses from surrounding irradiances formed a u-shaped pattern. For example, the two apparent low points in Figure 9 are at -4.2 and -3.7 log units attenuation. The stimulus consisted of a 480 nm stimulus flickered out-of-phase with a white light at a temporal frequency of 4.6 Hz. The selected isoluminant point in Figure 9 is marked with a circle. This value was chosen as the isoluminant point because, in addition to having the lowest response amplitude, the u-shaped pattern was comprised of a consistent decline before reaching the lowest point. The point at -4.2 log units attenuation could be due to variability rather than a change in visual effectiveness of the two stimuli since there are fewer points showing a declining trend to that point. The point circled in Figure 10 was not selected because it did not have the lowest amplitude and because the response amplitudes at surrounding irradiances did not produce as many points of decline in amplitude before reaching the minimum point. All decisions regarding the selection of the isoluminant point were made by two experimenters. The inverse of the selected irradiance measured in quanta/cm<sup>2</sup>/s corresponding to the isoluminant point was defined as the sensitivity of the subject to the test wavelength at the given flicker rate. Figure 11 shows several irradiance-response functions to 340, 420, 440, and 600 nm light (Figure 11a-d, respectively) flickered out-of-phase with a white light at a temporal rate of 4.6 Hz for an individual subject. The isoluminant points from Figures 11a-d were -1.0, -4.0, -

4.0, and -2.5 log units attenuation, respectively. The spectral sensitivity function of each fish was determined by plotting the sensitivity of the fish at each wavelength from the isoluminant points. Figure 12 shows the spectral sensitivity function for an individual fish. The sensitivity values determined from the irradiance-response functions in Figure 11 are highlighted with a circle and labelled relative to Figure 11 in Figure 12.

Sensitivity values at each wavelength and flicker frequency were averaged across fish.

Averaging was performed separately for the 4.6 and 16 Hz temporal rates. Spectral sensitivity data from two fish were omitted from the average spectral sensitivity functions because too few data points were collected. Only those subjects with 10 or more data points were included in analyses. Plotting each averaged sensitivity value across wavelength, spectral sensitivity functions for 4.6 Hz and 16 Hz stimuli were determined (see Figure 13 and Figure 14, respectively). The spectral sensitivity functions determined at the two flicker rates are shown together for comparison in Figure 15. It is clear that zebrafish are more sensitive to lower wavelengths of light than to higher wavelengths. In fact, at both temporal rates it is clear that subjects were more sensitive to ultraviolet than to the other wavelengths. To determine whether there were differences in sensitivity across temporal rates, a 2 x 12 (temporal rate x wavelength) repeated factors ANOVA was performed on the averaged data. Mean values were substituted for four missing data points from separate fish before analyses. The analysis showed a significant main effect of wavelength,  $F(11,99) = 7.48$ ,  $p = .005$ . Post hoc analysis demonstrated that, in general, zebrafish are more sensitive to lower wavelengths of light than to higher wavelengths ( $p < .05$ ). The analysis showed no significant difference between the two temporal rates,

$\underline{F}(1,9) = 3.52$ ,  $\underline{p} = .093$ . The interaction between temporal rate and wavelength also was not significant,  $\underline{F}(11,99) = 1.31$ ,  $\underline{p} = .230$ . Therefore, there was no apparent difference between the spectral sensitivity functions derived under the two temporal rates.

Cone modeling. The purpose of cone modeling was to determine the relative contribution of each of the four cone types to the spectral sensitivity functions derived under the two temporal rates. The model equation used was calculated based on a linear model (Coughlin & Hawryshyn, 1994; DeMarco & Powers, 1991) having the following form:

$$S_{\lambda} = (K_U * A_U) + (K_S * A_S) + (K_M * A_M) + (K_L * A_L)$$

where  $S_{\lambda}$  corresponds to the normalized sensitivity at wavelength  $\lambda$ ,  $K_X$  is the weighted coefficient for each cone type, and  $A_X$  is the normalized absorption at each wavelength  $\lambda$  for each cone type. The value of  $K_X$  can be positive or negative, where negative values suggest inhibition or chromatic opponency. In order to derive the best fit to the model, a nonlinear regression technique was used. The purpose of nonlinear regression is similar to that of linear regression which is to find the equation that accounts for the most variance in the data. To determine that, the software assigned weighted coefficients to each cone mechanism in the model based on its relative contribution to the spectral sensitivity functions from the data. The use of any modeling procedure requires that starting weights be estimated prior to running the analyses. Since the final weight values can depend on the initial values, several different starting weights were used to verify that the same final weights converged independently of the starting values. Based on preliminary analyses of this model, starting weights of 0.0 for all cone types yielded



reliable final values when compared to the model based on a variety of different starting weights. Therefore, starting weights of 0.0 were used for all cone types in the present modeling procedure.

Absorption spectra ( $A_x$ ) were derived for each cone type from the Dartnall nomogram for rhodopsin (Knowles & Dartnall, 1977). The rhodopsin nomogram was used for zebrafish rather than the porphyropsin (which is usually found in freshwater fish) nomogram based on its goodness of fit (porphyropsin  $\chi^2=13.09$ ;  $df=13$ ;  $p<.50$ ; rhodopsin  $\chi^2=2.54$ ;  $df=13$ ;  $p<.99$ ) with the MSP absorption spectra of the U-cone type provided by Robinson et al., (1993). By using the nomogram, the approximate absorptance of any cone type can be determined across other wavelengths given any peak wavelength. The shapes of the absorptance spectra for different cone types, when placed on a frequency rather than wavelength scale, are very similar in shape (Knowles & Dartnall, 1977). Nomogram curves were shifted laterally on a frequency scale to align with the  $\lambda_{max}$  for each cone type reported by Robinson et al. (1993). An eighth order polynomial equation (Flamarique & Hawryshyn, 1996) was found which best fit the absorptance spectra data for each of the zebrafish cone types. From the equations determined above, the percent absorptance of each of the cone types to the wavelengths tested in the present study was determined. The absorptance values were converted to proportions and normalized with respect to its maximum value. Spectral sensitivity values for individual fish were converted to proportions and normalized with respect to its maximum value at each temporal rate (see DeMarco & Powers, 1991). Mean values were substituted for three missing values from separate fish. Using a least squares nonlinear regression software

package (Data Most Corporation, Salt Lake City, UT, Stat-Most, ver. 2.5), the relative contribution of each cone type to the spectral sensitivities under the two temporal rates was determined. Table 1 shows the weighted coefficients for each cone type determined for the temporal rates of 4.6 Hz and 16 Hz for each fish as well as for the average spectral sensitivity functions across all fish. Also included are the sums of squares of the model for each fish and the averaged spectral sensitivity functions to both temporal rates.

Figure 16 and Figure 17 show the averaged data (filled squares) to 4.6 Hz and 16 Hz stimuli across all fish as well as the best fit model (solid line) corresponding to the weighted coefficients. In general, the models based on the final weights do not represent a good fit to the data. First, the sums of squares between the model and the actual data are relatively high; typical values are below 0.30 (e.g., see Flamarique & Hawryshyn, 1996). In addition, by comparing the model and the data in Figure 17, a large discrepancy can be seen, especially at 520 nm. The sum of squares for the 4.6 Hz model (0.54) is greater than for the 16 Hz model (0.31), possibly suggesting that the model of the data derived to 4.6 Hz flicker does not fit the data as well as the 16 Hz model. A 2 x 4 (temporal rate x cone type) repeated factors ANOVA was performed on the cone weights. The analysis showed that differences in weights between the two temporal rates was not significant,  $F(1,9) = 0.02$ ,  $p = .883$ . Also, the interaction of temporal rate and cone type was not significant,  $F(3,27) = .06$ ,  $p = .982$ . Note, however, that in both spectral sensitivity functions that there is a strong contribution of the U-cones; this implies a strong contribution of the U-cones to the spectral sensitivity function under both temporal rates.

### Temporal Properties of the Cone Inputs

Temporal response. The temporal response for each cone type was determined for nine zebrafish. One of these subjects was also a subject in the HFP procedure. The temporal response to flicker was derived from the Fourier amplitude of the fundamental component of the ERG b-wave response. This temporal response was determined for each of the four cone types of the zebrafish. In the present experiment, chromatic adaptation was used to separate the functioning of individual cone types. This procedure was accomplished by exposing the subject to a monochromatic background chosen to selectively adapt each cone type (see Temporal response procedure above and Chromatic adaptation verification section below).

All ERG responses were filtered and subjected to Fourier decomposition as previously described in the ERG signal averaging results section. To ensure that the responses across conditions were comparable, response amplitudes were standardized within test wavelength for each fish--that is, the highest response amplitude was divided by the response amplitudes of the other temporal rates under each condition. The log of each of these values was then plotted by stimulus temporal rate. Figure 18 shows the log relative response amplitude of each of the cone types averaged across fish. The temporal responses of the four cone types are similar except at temporal rates of 16 Hz and higher. At the temporal rate of 24 Hz, it appears that the relative response amplitudes begin to flatten.

To determine whether there were significant differences between the cone types, a 4 x 7 (cone type x temporal rate) repeated factors ANOVA was performed on the

temporal response data. The analysis showed a significant main effect of cone type,  $F(3,24) = 4.76$ ,  $p = .01$ , and a significant main effect of temporal rate,  $F(6,48) = 119.76$ ,  $p < .001$ . A significant interaction between cone type and temporal rate was also revealed,  $F(18,144) = 4.28$ ,  $p < .001$ . Simple effects analyses were conducted across cone types for each temporal rate. A probability of less than .001 was selected for all simple effects analyses. Simple effects analyses showed a significant difference between cone types at the temporal rates of 16 Hz,  $F(3,144) = 8.825$ , 20 Hz,  $F(3,144) = 15.0$ , and 24 Hz,  $F(3,144) = 6.425$ . To assess differences between the cone types at those temporal frequencies, Tukey's HSD analyses were conducted. All significant results from the Tukey's HSD analyses are reported at an alpha level of .05. At the temporal rate of 16 Hz, the U-cones respond significantly more than the S-, M-, or L-cone types,  $d_{crit}(4,24) = .26$ . Analysis of the cone types at 20 Hz showed that the L-cones responded significantly less than the U-, S-, or M-cone types  $d_{crit}(4,24) = .34$ . Finally, at 24 Hz, analyses revealed that the U-cones responded significantly more than the M- and L-cone types  $d_{crit}(4,24) = .26$ . Figure 19 shows the log relative response amplitude of each of the four cone types at the flicker rates eliciting significant differences between cone type responses.

Chromatic adaptation verification. To determine the effectiveness of the adaptation background to selectively adapt the individual cone responses, spectral sensitivity values from one fish were derived via an increment threshold technique. In this procedure, sensitivity is derived by determining the stimulus irradiance which produces a criterion response. In this case, the criterion response was a b-wave amplitude

of +50  $\mu\text{V}$  (see Hughes, 1996). In the increment threshold technique, the test stimulus is superimposed onto the background stimulus. This method of stimulus presentation differs from the HFP procedure where the test stimulus replaces the background stimulus. Figure 20 represents the sensitivity to different wavelengths of light after 10 min of adaptation to a white light (a), a 600 nm light (b), a 500 nm light (c), and a 440 nm (d). All background intensity values were 5  $\mu\text{W}/\text{cm}^2$ . Figure 20a shows the sensitivity of the zebrafish visual system to 360, 420, 480, and 640 nm light while being exposed to the white background light. This background condition was used to ensure that ERG responses were from cone rather than rod photoreceptors. By testing the visual system to 600 nm flicker under the white light background, it is assumed that the ERG responses reflect only the L-cone input. Therefore, even though the L-cone sensitivity may be lower than the other cone inputs (see Figure 20a), the L-cone type is the only cone type capable of responding to such a long wavelength of light (see Figure 1). Figure 20b shows sensitivity values during chromatic adaptation to 600 nm light. Under this background, only the L-cone responses are suppressed. Note that the sensitivity to the other wavelengths increases (compare Figure 20a with Figure 20b). By adapting to 600 nm light, it is assumed that the response threshold of the L-cones is reduced resulting in strongest contribution of the M-cones to a 500 nm test light. To obtain responses primarily from the S-cones, the response threshold of the M-cones must be increased. Figure 20c shows the sensitivity values while adapting to a 500 nm light. The sensitivity to 420 nm light is higher while the sensitivity to 480 nm light is lower compared to the values in Figure 20b. Responses of the S-cones are assumed to be contributing more than

the M-cones after adaptation under this condition to a 420 nm test stimulus. Finally, while adapting to 440 nm light, the sensitivity to 420 nm light is reduced. The response threshold of the S-cones is reduced allowing a stronger contribution of only U-cones to a 360 nm test light (see Figure 1).

## **Chapter 5**

### **Discussion**

#### Overview

Two main questions were investigated regarding the role of separation of visual processing in zebrafish. First, since the zebrafish has recently become an important vertebrate model for vision researchers, it is necessary to address the possibility that zebrafish process chromatic and visual stimuli through functionally separate pathways. It was hypothesized that zebrafish, like most vertebrate species, including other teleost fish, would demonstrate separation of visual processing. Secondly, the present research was intended to test the hypothesis that cone inputs with high temporal resolution would contribute to both visual channels while only those cone types with the lowest temporal resolution would provide inputs to the chromatic channel. By inference, the second hypothesis suggests that the luminance channel can be stimulated only by faster temporal stimuli compared to the chromatic channel. Thus, stimuli of high temporal frequency should only be encoded by cone types with high temporal resolution.

Results reported above demonstrate that the hypothesis that zebrafish process chromatic and luminance information through functionally separate visual channels was not supported. The spectral sensitivity curves derived with 4.6 and 16 Hz stimuli were not significantly different. Furthermore, the cone weights determined by modeling the cone responses did not significantly differ between the two temporal rates. The hypothesis that the temporal resolution of the cone inputs would be related to their

contributions to the separate processing of chromatic and luminance information was not fully supported since significant differences were found between the temporal resolution of the cone types while no significant differences were revealed between the spectral sensitivity functions determined by HFP with the two temporal rates examined.

However, other implications for the results of the temporal resolution investigation will be discussed in the temporal resolution discussion section.

### HFP

To determine which visual channel is represented by the spectral sensitivity functions determined by HFP, a number of results must be addressed. The mean weights from the cone modeling determined for both spectral sensitivity functions were positive (see Table 1). Since negative weights suggest chromatic inhibition, the modeling performed on the present data suggests that there is no chromatic inhibition at either 4.6 or 16 Hz. This finding suggests that the spectral sensitivity functions determined in the present study represent the spectral sensitivity of the luminance channel. Although there are both positive and negative weights for individual fish as seen in Table 1, these differences may be due to variability since there are no significant differences between the weights derived with 4.6 Hz and 16 Hz stimuli. In addition, when the weights were averaged at each temporal rate, any signs of inhibition were removed from the final equation. Since the inhibition “averaged out” of the final spectral sensitivity functions, there was no consistent pattern of inhibitory cone inputs that would suggest chromatic inhibition. However, observation of the spectral sensitivity functions, especially to 4.6 Hz stimuli, shows some notches or points of decreased sensitivity characteristic of



chromatic inhibition (see Figure 13). It is possible that the notches such as the one around 520 nm are a result of variability in the data; however, it is interesting to note that 520 nm is where a notch should occur if there were opponent contributions between the M- and L-cones (see Figure 1).

Research by a number of other researchers may offer an alternate explanation for the present findings based on methodological differences. Behavioral research by Neumeyer et al. (1991) has demonstrated functional separation of color and luminance processing in goldfish. Using an increment threshold technique where monochromatic stimuli were presented under different levels of room illumination, animals were found to show behavior suggesting that chromatic and luminance information were processed separately by the visual system. Similarly, Mackintosh et al. (1987) have demonstrated spectrally opponent and nonopponent ganglion cells in goldfish. They used chromatic adaptation to selectively suppress the responses of individual cone types. By suppressing individual cone types, the contributions of S-, M-, and L-cone types to the goldfish spectral sensitivity function were determined at different background intensities.

Unlike the goldfish, investigation of the zebrafish visual system has not addressed separate processing of temporal, spatial frequency, color, or luminance processing through anatomical, electrophysiological, or behavioral means. Unlike previous researchers who have found separation of processing using increment threshold techniques, Regan et al. (1975) found no opponency in goldfish ERG responses using HFP stimuli, the same method and response measure used in the present research. Regan et al. presented monochromatic light and white light out-of-phase at temporal rates of 2.5,

10, and 20 Hz and found no significant differences between the spectral sensitivity functions derived with each temporal rate. The results revealed only the presence of a luminance channel. Thus, it is clear that there is an inconsistency in goldfish regarding the presence of separate visual channels, as well. Present findings regarding the absence of a chromatic channel in zebrafish are consistent with the results reported by Regan et al. using HFP.

Previous research on the separation of color and luminance processing in higher vertebrates has demonstrated several processing characteristics of the two channels. Zrenner et al. (1990) summarize these findings reporting that the luminance channel typically is not sensitive to color discrimination or high spatial resolution, but rather has high contrast sensitivity and is sensitive to fast temporal stimuli. The color channel typically responds counter to the luminance channel. Since only one of these aspects of separate visual processing was assessed by the present study, it is possible that the zebrafish visual system does process information separately based on other stimulus characteristics associated with separation in higher vertebrates. However, recent research by Hughes (1996) using an increment threshold technique to determine if zebrafish exhibit separation of visual processing revealed color opponent processing in the ERG response. A careful comparison of the 4.6 Hz spectral sensitivity function in the present study with the chromatic channel spectral sensitivity function determined at approximately the same temporal rate by Hughes shows a great deal of similarity, especially at wavelengths between 320 and 420 nm where Hughes finds inhibitory S-cone input. Although there is a difference in sensitivity between the spectral sensitivity

functions at higher wavelengths across the two studies, the shape of the two functions is virtually the same. The notches and areas of peak sensitivity align very closely across wavelength. This similarity in shape is interesting considering the higher variability present in the HFP data.

Since separation of processing has been found in goldfish (Mackintosh et al., 1987; Neumeyer et al., 1991) and zebrafish (Hughes, 1996) using increment threshold techniques, while no separation has been found in the same species using HFP (Regan et al., 1987; the present study), it is possible that HFP does not provide a means by which to study the chromatic channel. The lack of inhibition demonstrated by cone modeling in the present study as well as the statistical insignificance between spectral sensitivity functions determined with 4.6 and 16 Hz flicker also may be a result of increased variability due to the HFP methodology, particularly at 4.6 Hz where a chromatic channel would most likely exist. The spectral sensitivity functions determined by Hughes, although similar in shape to those in the present study, had less variability in the data. The fact that Regan et al. (1975) did not find opponency in goldfish using HFP may be a characteristic result of determining spectral sensitivity with HFP. It seems that increment threshold may be more sensitive for determining the spectral sensitivity functions of chromatic channels. The use of HFP may be less sensitive to chromatic inhibition which may account for the present findings.

It is also possible that zebrafish process all visual information through one channel. Livingstone and Hubel (1988) suggest that only the processing of luminance information is necessary for the location of food, the escape from predators, and other

visual tasks necessary for survival. Present findings do support the assertions by Livingstone and Hubel that the luminance channel is more primitive and the most basic form of visual processing necessary for survival.

### Temporal Response

The present study shows that there are some differences in the temporal resolution of the four zebrafish cone types. The hypothesis that zebrafish cone inputs to the separate processing channels would be based on their temporal resolution was not fully supported. Since there appears to be no separation of visual processing based on the temporal rates investigated by the present study, any difference in temporal resolution between the cone types is contrary to the hypothesis. However, upon closer analysis of the temporal response results, the spectral sensitivity functions determined by HFP are consistent. At temporal rates slower than 16 Hz, there were no significant differences between the cone types. At 16 Hz, however, analyses showed that the U-cones had significantly higher temporal resolution than the other three cone types. At 20 Hz, the L-cones were significantly slower in temporal resolution than the other cone types. Finally, at 24 Hz, the U-cones responded significantly more than the L- and M-cone types. Taken together, these results are consistent with the spectral sensitivity functions to both 4.6 Hz and 16 Hz. As can be seen in Figure 14, the spectral sensitivity functions show highest sensitivity in the range of wavelengths between 320 nm to 420 nm. Similarly, the zebrafish is least sensitive to wavelengths above 520 nm. Analyses of temporal response data demonstrate that the U-cone type has the highest temporal resolution. This increased temporal rate may be partly responsible for the increased sensitivity of the zebrafish to

ultraviolet wavelengths. Conversely, the L-cones appear to have the slowest temporal resolution which may be responsible for the decreased sensitivity to long wavelengths of light.

### Implications of the Present Study

As previously mentioned, Livingstone and Hubel (1988) suggest that the luminance channel is required for basic survival. It is consistent that if the zebrafish possess only one visual channel, it is the luminance channel. However, unlike the luminance channels of other vertebrate species including humans (Boynton, 1979), primates (Zrenner et al., 1990), tree shrews (Petry, 1993), and goldfish (Regan et al., 1975) which have greatest sensitivity to long and middle wavelengths, the zebrafish luminance channel clearly has greatest sensitivity to ultraviolet and short wavelengths of light (see Figure 14). Robinson et al. (1993) report that 25% of the cone mosaic in zebrafish is comprised of U-cones which explains their high sensitivity to ultraviolet wavelengths in the present study. This representation of U-cones in the cone mosaic is uncommon, even in other species which demonstrate sensitivity to ultraviolet wavelengths. In addition to anatomical evidence, the present research is the first to provide physiological evidence of the high sensitivity of the zebrafish visual system to ultraviolet wavelengths. It is speculated that this difference in sensitivity is a result of the different visual environment in which the zebrafish originates. It is possible that their breeding and feeding territory in the Ganges river (Barinaga, 1990) necessitates high ultraviolet sensitivity. In captivity and in the natural environment, zebrafish swim most of the time near the surface of the water where ultraviolet light easily penetrates. At

shallow depths, ultraviolet sensitivity would greatly enhance the visual ability of these animals. Other teleost fish including the Atlantic salmon (Kunz et al., 1994) and the rainbow trout (Browman & Hawryshyn, 1994) possess U-cones as young fish when they dwell near the surface of the water but lose ultraviolet sensitivity as adults when they migrate to deeper water.

Although past research on a number of species including macaques (DeValois et al., 1966; Schiller & Malpelli, 1978 ), other primates (Kremers et al., 1992; Lee et al., 1990; Schiller & Logothetis, 1990; Schiller & Malpelli, 1978 ) and cats (Enroth-Cugell & Robson, 1966; Hochstein & Shapley, 1976) has shown that higher vertebrates process visual information through separate anatomical pathways, studies involving lower vertebrates like goldfish have not been so clear. Anatomical and physiological research with goldfish has demonstrated separation of on and off pathways in the visual system (see DeMarco & Powers, 1991). It is possible that the anatomical separation of on and off pathways is more fundamental to the teleost visual system and allows for the separation of visual pathways along separate stimulus parameters. However, anatomical research on goldfish and other teleosts has not shown separation of color and luminance processing. Electrophysiological investigation of goldfish ganglion cells by Bilotta and Abramov (1989) have revealed that temporal properties of the cells can influence their spatial processing. Mackintosh et al. (1987) and Gouras and Zrenner (1979) have demonstrated cells in goldfish and primates that accommodate functional separation in the absence of anatomically separate pathways. Mackintosh et al. (1987) found that by presenting lights of intensities well above response threshold, normally spectrally

opponent cells exhibited spectrally nonopponent characteristics. Findings by Gouras and Zrenner (1979) showed that cells presented with lights flickering at high temporal rates underwent a response phase shift between center and surround mechanisms causing normally spectrally opponent cells to exhibit spectrally nonopponent characteristics. From these findings, it is clear that mechanisms exist to accommodate separation of processing based on different characteristics of visual stimuli in at least two species. The presence of these cellular mechanisms suggest that separation of processing exists at a basic level in the visual system. That these mechanisms did not become apparent in the zebrafish visual system is unusual. However, as previously stated, the absence of separation found by the present study may be due to methodological rather than functional deficiencies. The present research should not be used as conclusive evidence that separation of visual function is not a fundamental component of vertebrate vision.

#### Future Directions

It is possible that the present research did not fully address the temporal characteristics of the zebrafish visual system. Different results may be produced if lower temporal rates are used to elicit responses from a color channel. Gouras and Zrenner (1979) have demonstrated that receptive fields may undergo a frequency dependent phase shift in response to temporal stimuli producing luminance-like functioning. The flicker rate of 4.6 Hz used in the present study may have been sufficiently high enough to cause receptive fields in the zebrafish visual systems to undergo the phase shift if such mechanisms exist in the zebrafish visual system. A lower temporal rate may produce a spectral sensitivity function that is different from those reported in the present research.

However, this phase shift does not occur in the goldfish visual system until between the temporal frequencies of 8 to 16 Hz (Bilotta & Abramov, 1989).

Although most isoluminant points were consistently selected by two experimenters, it is possible that the use of different selection criteria could produce different results. However, the selection criteria used in the present study were used in previous research (Regan et al., 1975). Future research should address analyzing the waveforms of individual ERG responses. Close analysis of the averaged ERG waveforms to 4.6 and 16 Hz stimuli may allow for a more accurate determination of isoluminant points. By analyzing waveforms of individual ERG responses, it may be possible to more accurately determine the irradiance at which the monochromatic and white stimuli reverse their visual effectiveness. By analyzing individual waveforms of the ERG responses, it may be possible to improve the selection of isoluminant points.

It is possible that testing the temporal response to higher temporal rates would further separate the temporal resolution of the U-cones from the other cone types. Future research should consider testing the temporal response of each cone type until the ERG response rate cannot follow the presentation rate of the stimuli. By testing each cone type until their response rate cannot follow the response rate of a stimulus, a more clear separation of temporal resolution may be discovered. If it was determined that there were clear differences between the cone types, such results could lend further support to the possibility that zebrafish do possess separate visual processing not efficiently elicited by HFP.



This research represents one of the first attempts to measure the ERG response from zebrafish. It has provided some interesting results regarding the use of HFP stimuli, the separation of chromatic and luminance processing and the high sensitivity of the zebrafish to ultraviolet light. Although future work will be necessary to address other questions about the zebrafish visual system, it is clear that the zebrafish is an appropriate and interesting model for vertebrate vision.

## References

- Barinaga, M. (1990). Zebrafish swimming into the development mainstream. Science, 250, 34-35.
- Bilotta, J., & Abramov, I. (1989). Spatial properties of goldfish ganglion cells. Journal of General Physiology, 93, 1147-1169.
- Bilotta, J., DeMarco, P. J., LaJoie, A. S., Dieckmann, C. M., Chatman, S. J., & Cosby, S. E. (1994). Heterochromatic flicker photometry in goldfish. Investigative Ophthalmology & Visual Science, 35 (Suppl.), 2168.
- Boynton, R. M. (1979). Human Color Vision. New York: Holt, Rinehart, and Winston.
- Brockerhoff, S. E., Hurley, J.B., Janssen-Bienhold, U., Neuhauss, S.C.F., Driever, W., & Dowling, J.E. (1995). A behavioral screen for isolating zebrafish mutants with visual system defects. Proceedings of the National Academy of Science, USA, 92, 10545-10549.
- Browman, H. I., & Hawryshyn, C. W. (1994). The developmental trajectory of ultraviolet photosensitivity in rainbow trout is altered by thyroxine. Vision Research, 34, 1397-1406.
- Clark, D. T. (1981). Visual responses in developing zebrafish (*Brachydanio rerio*). Unpublished doctoral dissertation, University of Oregon, Eugene.

Coughlin, D. J., & Hawryshyn, C. W. (1994). The contribution of ultraviolet and short-wavelength sensitive cone mechanisms to color vision in rainbow trout. Brain Behavior and Evolution, 43, 219-232.

DeMarco, P. J., & Powers, M. K. (1991). Spectral sensitivity of ON and OFF responses from the optic nerve of goldfish. Visual Neuroscience, 6, 207-217.

DeValois, R. L., Abramov, I., & Jacobs, G. H. (1966). Analysis of response patterns of LGN cells. Journal of the Optical Society of America, 56, 966-977.

Eisner, A., & MacLeod, D. I. A. (1980). Blue sensitive cones do not contribute to luminance. Journal of the Optical Society of America, 70, 121-123.

Enroth-Cugell, C., & Robson, J. G. (1966). The contrast sensitivity of retinal ganglion cells of the cat. Journal of Physiology, 187, 517-552.

Flamarique, I.N., & Hawryshyn, C.W. (1996). Retinal development and visual sensitivity of young Pacific sockeye salmon (*Oncorhynchus nerka*). Journal of Experimental Biology, 199, 869-882.

Gouras, P., & Zrenner, E. (1979). Enhancement of luminance flicker by color-opponent mechanisms. Science, 205, 587-589.

Gregory, R. L. (1981). Eye and brain: The psychology of seeing (3rd ed.). New York: McGraw Hill Book Company.

Hanitzsch, R., Lichtenberger, T., & Mattig, W. U. (1996). The influence of  $MgCl_2$  and APB on the light-induced potassium changes and the ERG b-wave of the superfused rat retina. Vision Research, 36, 499-507.

Hartline, H. K. (1938). The response of single optic nerve fibers of the vertebrate eye to illumination of the retina. American Journal of Physiology, 121, 400-415.

Hergenhahn, B. R. (1992). An introduction to the history of psychology (2nd ed.). Belmont, CA: Wadsworth Publishing Company.

Hochstein, S., & Shapley, R. M. (1976). Quantitative analysis of retinal ganglion cell classifications. Journal of Physiology, 262, 237-264.

Hughes, R.A. (1996). Determination of chromatic and luminance channels in the zebrafish using an increment threshold technique. Unpublished master's thesis, Western Kentucky University.

Hurvich, L. M., & Jameson, D. (1957). An opponent-process theory of color vision. Psychological Review, 64, 384-404.

Kalat, J. W. (1992). Biological Psychology (4th ed.). Belmont, CA: Wadsworth Publishing Company.

King-Smith, P. E., & Carden, D. (1976). Luminance and opponent color contributions to visual detection and adaptation to temporal and spatial integration. Journal of the Optical Society of America, 66, 709-717.

Knowles, A., & Dartnall, H. J. A. (1977). Spectroscopy of visual pigments. In H. Davson (Ed.), The Eye, v. 2B (pp. 74-84). Academic Press: New York.

Kremers, J., Lee, B. B., & Kaiser, P. K. (1992). Sensitivity of macaque retinal ganglion cells and human observers to combined luminance and chromatic temporal modulation. Journal of the Optical Society of America, 9, 1477-1485.

Kuffler, S. W. (1953). Discharge patterns and functional organization of mammalian retina. Journal of Neurophysiology, 16, 37-68.

Kunz, Y. W., Wildenburg, G., Goodrich, L., & Callaghan, E. (1994). The fate of ultraviolet receptors in the retina of the Atlantic Salmon (*Salmo salar*). Vision Research, 34, 1375-1383.

Lee, B. B., Martin, P. R., & Valberg, A. (1988). The physiological basis of heterochromatic flicker photometry demonstrated in the ganglion cells of the macaque retina. Journal of Physiology, 404, 323-347.

Lee, B. B., Pokorny, J., Smith, V. C., Martin, P. R., & Valberg, A. (1990). Luminance and chromatic modulation sensitivity of macaque ganglion cells and human observers. Journal of the Optical Society of America, 7, 2223-2236.

Levine M. W., & Shefner, J. M. (1991). Fundamentals of Sensation and Perception (2nd ed.). Reading, MA: Addison-Wesley Publishing Company.

Livingstone, M., & Hubel, D. (1988). Segregation of form, color, movement, and depth: Anatomy, physiology, and perception. Science, 240, 740-749.

Loop, M. S., Millican, C. L., & Thomas, S. R. (1987). Photopic spectral sensitivity of the cat. Journal of Physiology, 382, 537-553.

Mackintosh, R. M., Bilotta, J., & Abramov, I. (1987). Contributions of short-wavelength cones to goldfish ganglion cells. Journal of Comparative Physiology A, 161, 85-94.

Nawrocki, L., Bremiller, R., Streisinger, G., & Kaplan, M. (1985). Larval and adult visual pigments of the zebrafish, *Brachydanio rerio*. Vision Research, 25, 1569-1576.

Neumeyer, C., Wietsma, J. J., & Spekreijse, H. (1991). Separate processing of “color” and “brightness” in goldfish. Vision Research, 31, 537-549.

Petry, H.M. (1993). Long-term changes in visual mechanisms following differential stimulation of color and luminance channels during development. Progress in Brain Research, 95, 235-250.

Powers, M. K., & Easter, S. S., Jr. (1983). Behavioral significance of retinal structure and function in fishes. In R.G. Northcutt and R.E. Davis (Eds.), Fish Neurobiology, v.1 (pp. 377-404). The University of Michigan Press: Ann Arbor.

Regan, D., Schellart, N. A. M., Spekreijse, H., & van den Berg, T. J. T. P. (1975). Photometry in goldfish by electrophysiological recording: Comparison of criterion response method with heterochromatic flicker photometry. Vision Research, 15, 799-807.

Robinson, J., Schmitt, E. A., & Dowling, J. E. (1995). Temporal and spatial patterns of opsin gene expression in zebrafish (*Danio rerio*). Visual Neuroscience, 12, 895-906.

Robinson, J., Schmitt, E. A., Harosi, F. I., Reece, R. J., & Dowling, J. E. (1993). Zebrafish ultraviolet visual pigment: Absorption spectrum, sequence, and localization. Proceedings of the National Academy of Science, USA, 90, 6009-6012.

Schiller, P. H., & Logothetis, N. K. (1990). The color-opponent and broad-band channels of the primate visual system. Trends in Neuroscience, 13, 392-398.

Schiller, P. H., & Malpelli, J. G. (1978). Functional specificity of lateral geniculate laminae of the rhesus monkey. Journal of Neurophysiology, 41, 788-797.

Sekuler, R., & Blake, R. (1994). Perception (3rd ed.). New York: McGraw-Hill, Inc.

Vennat, J.C., Besse, G., Sanzelle, S., Doly, M., & Gaillard, G. (1994). A program for automatic acquisition and processing of electroretinograms obtained in vivo in albino rats. Journal of Neuroscience Methods, 52, 17-21.

Zrenner, E., Abramov, I., Akita, M., Cowey, A., Livingstone, M., & Valberg, A. (1990). Color perception: Retina to cortex. In Visual Perception: The Neurophysiological Foundations. (pp.163-202). New York: Academic Press.

Table 1

Cone weights of individual subjects at 4.6 Hz and 16 Hz

|         | <u>Temporal Rate</u> |       |       |       |      |       |       |       |       |      |
|---------|----------------------|-------|-------|-------|------|-------|-------|-------|-------|------|
|         | 4.6 Hz               |       |       |       |      | 16 Hz |       |       |       |      |
| Subject | U                    | S     | M     | L     | SS   | U     | S     | M     | L     | SS   |
| AC      | .543                 | .038  | -.091 | .230  | .522 | .153  | .022  | .038  | .032  | .929 |
| AD      | .179                 | -.006 | .045  | .027  | .920 | .532  | -.057 | .020  | -.019 | .496 |
| AF      | .550                 | -.094 | .020  | -.016 | .479 | .352  | .594  | -.084 | .009  | .711 |
| AG      | .210                 | -.018 | .053  | .026  | .910 | .356  | -.070 | .059  | .001  | .765 |
| AH      | .164                 | .345  | -.026 | .105  | 1.22 | -.277 | .627  | -.064 | .111  | .332 |
| AI      | .325                 | .145  | .023  | .399  | .793 | -.096 | -.246 | .869  | .045  | .101 |
| AJ      | -.204                | .576  | -.048 | .022  | .465 | .299  | .183  | .052  | .059  | .973 |
| AK      | .693                 | .028  | .042  | -.012 | .495 | .477  | .110  | .003  | -.007 | .532 |
| AO      | .874                 | -.115 | .091  | .008  | .538 | .562  | -.084 | .020  | -.017 | .451 |
| AT      | -.240                | .678  | .362  | .022  | .338 | .689  | .153  | -.064 | .574  | .553 |
| Mean    | .790                 | .0001 | .064  | .017  | .541 | .601  | .074  | .061  | .004  | .313 |

Note. U=ultraviolet cones, S=short cones, M=middle cones, L=long cones, SS= sum of squares. Mean represents the weights of each cone type averaged across 10 fish.



### Figure Captions

Figure 1. Log relative absorptance of the four cone types as a function of wavelength fitted from the rhodopsin nomogram. The solid line represents the absorptance of U-cones ( $\lambda_{\max} = 362$  nm), the dashed line represents the log relative absorptance of the S-cones ( $\lambda_{\max} = 420$  nm), the dash-dotted line represents the log relative absorptance of the M-cones ( $\lambda_{\max} = 480$  nm), and the dash-double dotted line represents the log relative absorptance of the L-cones ( $\lambda_{\max} = 570$  nm). See text for details

Figure 2. Unfiltered ERG responses to heterochromatic flicker collected from subject AT. The 440 nm light at -2.0 log units attenuation (0.0 log attenuation = 12.89 quanta/cm<sup>2</sup>/s) was flickered out-of-phase with a 5.22  $\mu$ W/cm<sup>2</sup> white light stimulus. The temporal rates were 4.6 Hz (a) and 16 Hz (b).

Figure 3. Filtered ERG responses to heterochromatic flicker collected from subject AT. Filtering removed 60 Hz AC noise riding on the ERG response. The 440 nm light was flickered out-of-phase with a 5.22  $\mu$ W/cm<sup>2</sup> white light stimulus. The temporal rates were 4.6 Hz (a) and 16 Hz (b).

Figure 4. One thousand millisecond segment of the filtered ERG response presented in Figure 3b. The sixteen ERG responses during this time are separated by vertical dashed lines. See Figure 3 for other details.

Figure 5. Averaged ERG responses collected from subject AT. Individual ERG responses from a 4000 ms presentation of 440 nm light flickered out-of-phase with a 5.22  $\mu$ W/cm<sup>2</sup> white light stimulus. The temporal rates were 4.6 Hz (a) and 16 Hz (b). The arrows indicate the change of stimuli from white light to the 440 nm test stimulus.

Figure 6. ERG responses collected from subject AT at three different test stimulus irradiances. ERG trains are in response to a 420 nm light at -2.0 log units attenuation (a), -2.5 log units attenuation (b), and -4.5 log units attenuation (c) flickering out-of-phase with a white light of  $5.22 \mu\text{W}/\text{cm}^2$  at 4.6 Hz. ERG responses in these panels demonstrate the increased effectiveness to monochromatic light compared to the white light (a), equal effectiveness of the white light and the monochromatic light representing the isoluminant point (b), and increased effectiveness of the white light compared to the monochromatic light (c) as the intensity of the monochromatic stimulus is decreased.

Figure 7. Irradiance-response function of subject AT to heterochromatic flicker. The 420 nm stimuli were flickered out-of-phase with a white light of  $5.22 \mu\text{W}/\text{cm}^2$  across log relative irradiances between -2.5 and -6.5 log units attenuation (0.0 log irradiance at 420 nm =  $12.81 \text{ quanta}/\text{cm}^2/\text{s}$ ) at 4.6 Hz. Response amplitude is the amplitude of the Fourier fundamental component.

Figure 8. Irradiance-response function of subject AT to heterochromatic flicker. The 520 nm stimuli were flickered out-of-phase with a white light of  $5.22 \mu\text{W}/\text{cm}^2$  across log relative irradiances between -1.5 and -5.0 log units attenuation (0.0 log irradiance at 520 nm =  $13.02 \text{ quanta}/\text{cm}^2/\text{s}$ ) at 16 Hz. Response amplitude is the amplitude of the Fourier fundamental component.

Figure 9. Irradiance-response function of subject AT to heterochromatic flicker. The 480 nm stimuli were flickered out-of-phase with a white light of  $5.22 \mu\text{W}/\text{cm}^2$  across log relative irradiances between -2.5 and -5.5 log units attenuation (0.0 log irradiance at 480 nm =  $13.02 \text{ quanta}/\text{cm}^2/\text{s}$ ) at 4.6 Hz. The circled point is the response amplitude corresponding to the log relative irradiance selected as the isoluminant point. Response amplitude is the amplitude of the Fourier fundamental component.

Figure 10. Irradiance-response function of subject AT to heterochromatic flicker. The 480 nm stimuli were flickered out-of-phase with a white light of  $5.22 \mu\text{W}/\text{cm}^2$  across log relative irradiances between -2.5 and -5.5 log units attenuation (0.0 log irradiance at 480 nm =  $13.02 \text{ quanta}/\text{cm}^2/\text{s}$ ) at 4.6 Hz. The circled point is the response amplitude corresponding to the log relative irradiance not selected as the isoluminant point (see text for details). Response amplitude is the amplitude of the Fourier fundamental component.

Figure 11. Irradiance-response functions of subject AT to test stimuli flickered out-of-phase with a white light of  $5.22 \mu\text{W}/\text{cm}^2$  at 4.6 Hz. Irradiance-response functions are in response to 340 nm stimuli (a) (0.0 log irradiance at 340 nm =  $11.74 \text{ quanta}/\text{cm}^2/\text{s}$ ) 420 nm stimuli (b) (0.0 log irradiance at 420 nm =  $12.81 \text{ quanta}/\text{cm}^2/\text{s}$ ) 440 nm stimuli (c) (0.0 log irradiance at 440 nm =  $12.89 \text{ quanta}/\text{cm}^2/\text{s}$ ) and 600 nm stimuli (d) (0.0 log irradiance at 600 nm =  $12.95 \text{ quanta}/\text{cm}^2/\text{s}$ ). Response amplitude is the amplitude of the Fourier fundamental component.

Figure 12. Spectral sensitivity function of subject AT to 4.6 Hz heterochromatic flicker stimuli. The circled points are sensitivity values derived from isoluminant points shown in Figure 11.

Figure 13. Spectral sensitivity function averaged across 10 fish to 4.6 Hz stimuli. Error bars represent  $\pm 1$  SEM.

Figure 14. Spectral sensitivity function averaged across 10 fish to 16 Hz stimuli. Error bars represent  $\pm 1$  SEM.

Figure 15. Averaged spectral sensitivity functions to 4.6 Hz (squares) and to 16 Hz (triangles) stimuli. Error bars represent  $\pm 1$  SEM.

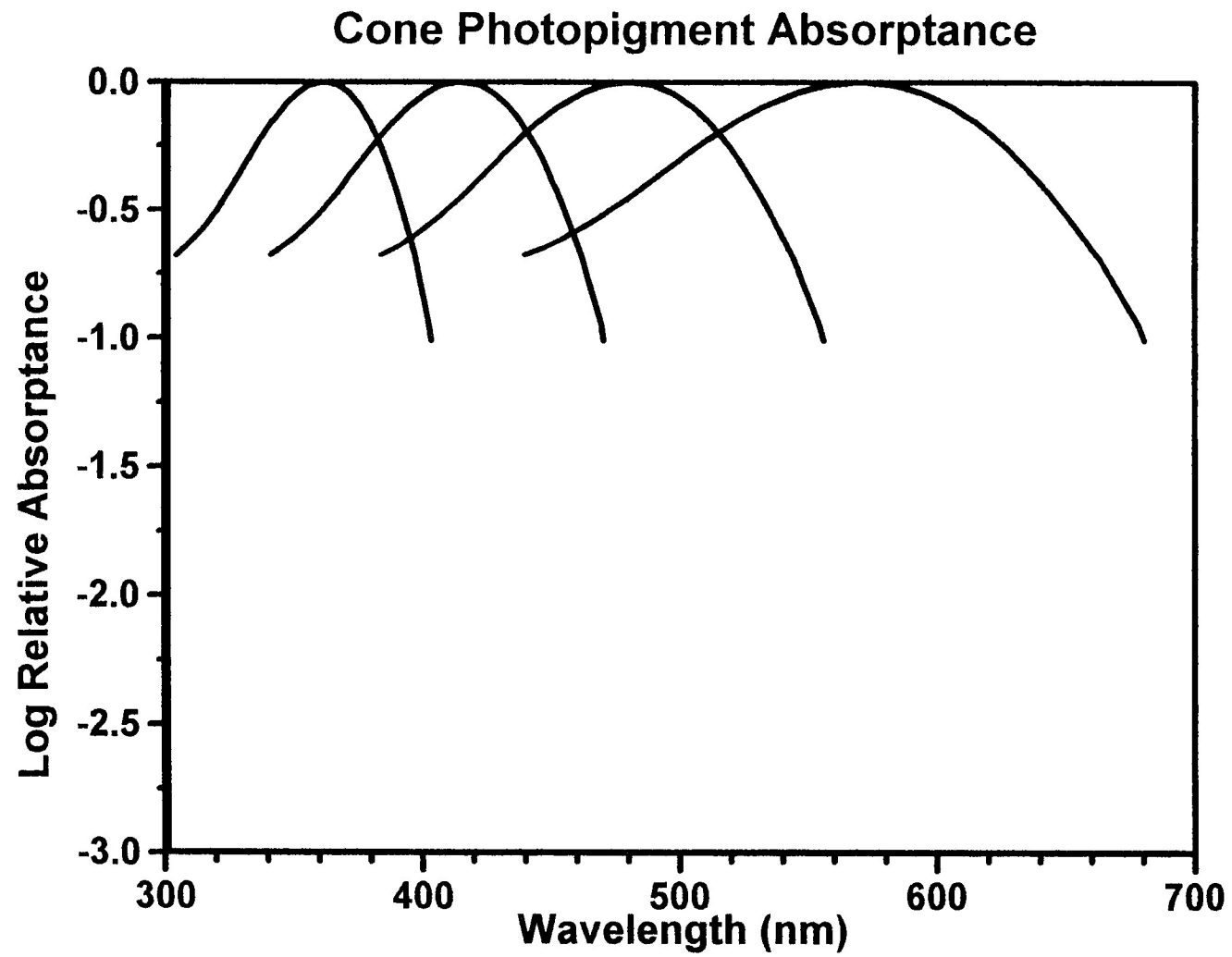
Figure 16. Averaged spectral sensitivity function to 4.6 Hz stimuli and modeled spectral sensitivity function based on cone inputs. The model is shown by the solid line and the data is shown by the squares. The final model weights also are shown.

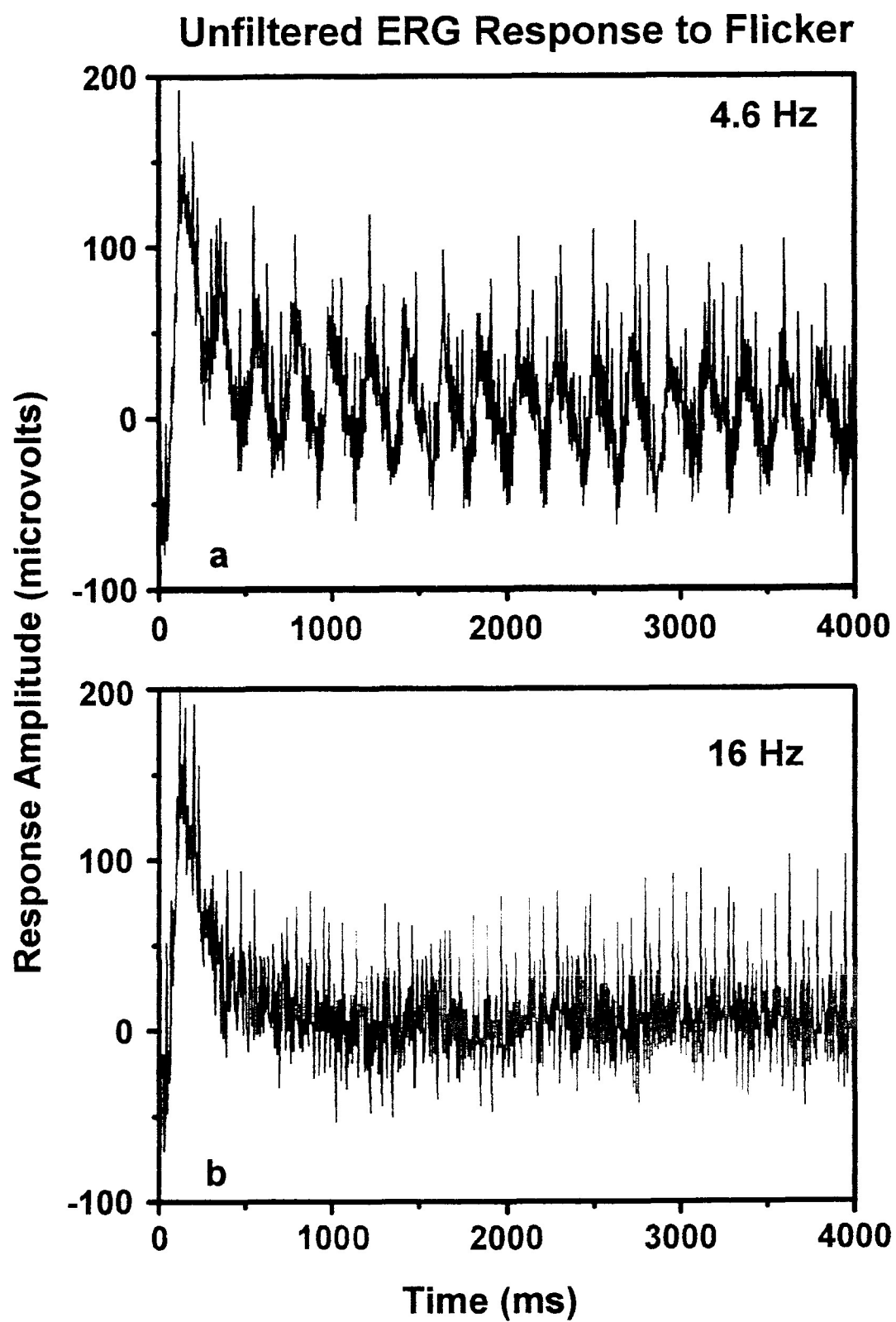
Figure 17. Averaged spectral sensitivity function to 16 Hz stimuli and modeled spectral sensitivity function based on cone inputs. The model is shown by the solid line and the data is shown by the squares. The final model weights also are shown.

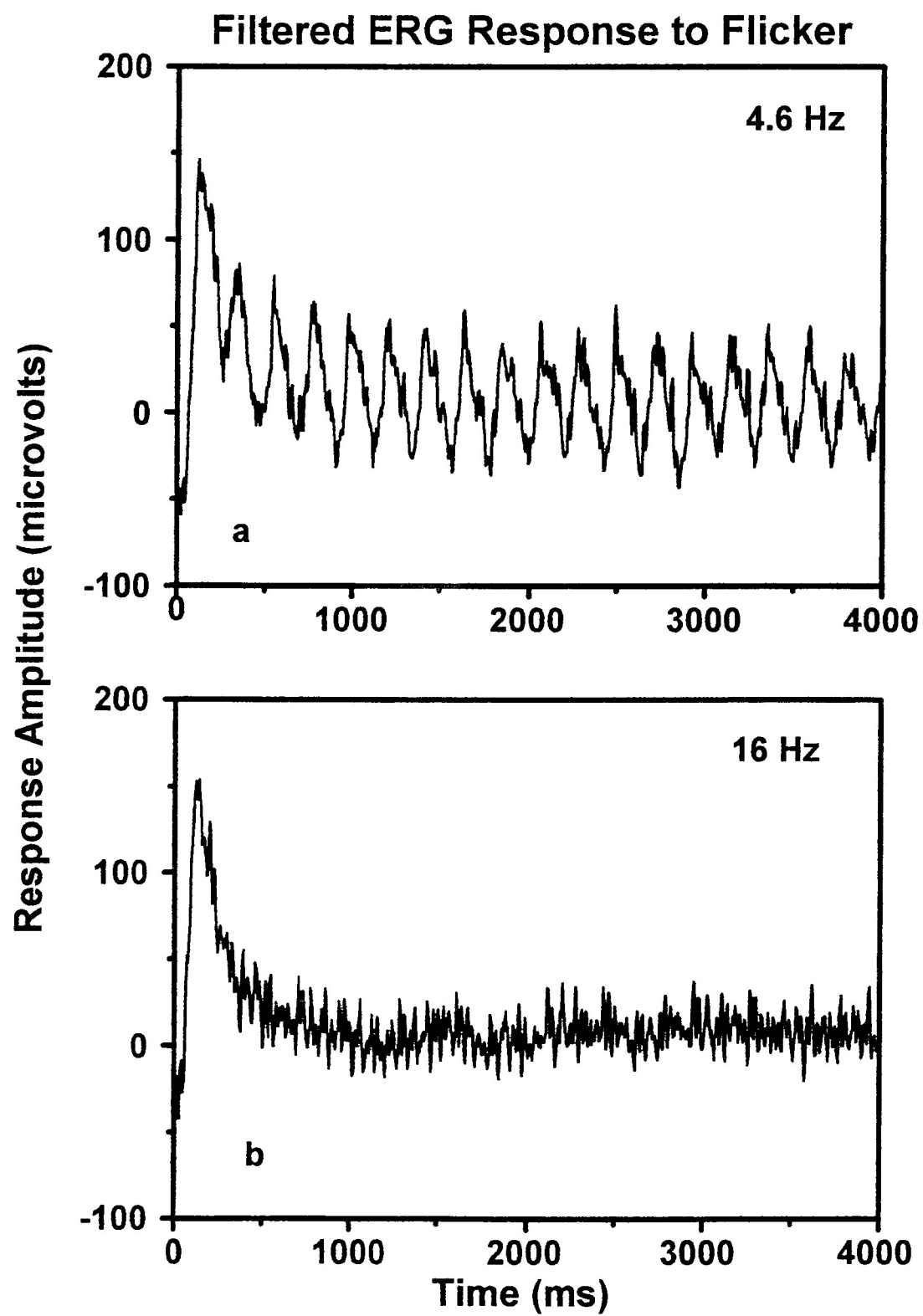
Figure 18. Temporal response function of U- (stars), S- (diamonds), M- (circles), and L- (triangles) cone types.

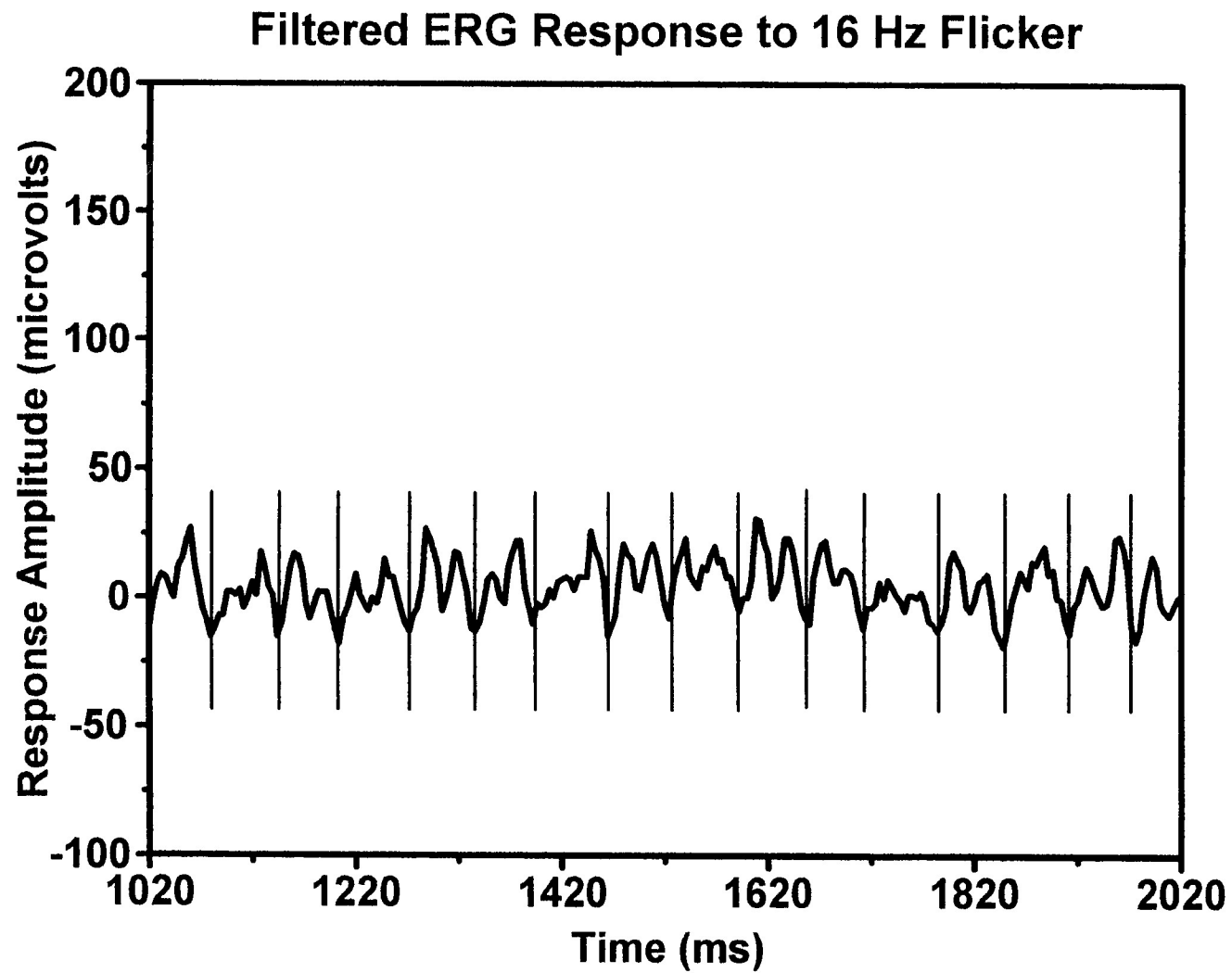
Figure 19. Cone temporal response amplitudes to 16 Hz (a), 20 Hz (b), and 24 Hz (c) stimuli during chromatic adaptation. See text for details.

Figure 20. Sensitivity to different wavelengths of light after 10 min chromatic adaptation to a white light (a), 600 nm light (b), 500 nm light (c), and 440 nm light. These four background conditions were used to isolate the L-, M-, S-, and U-cone type inputs (Figure a, b, c, and d, respectively); see text for details.





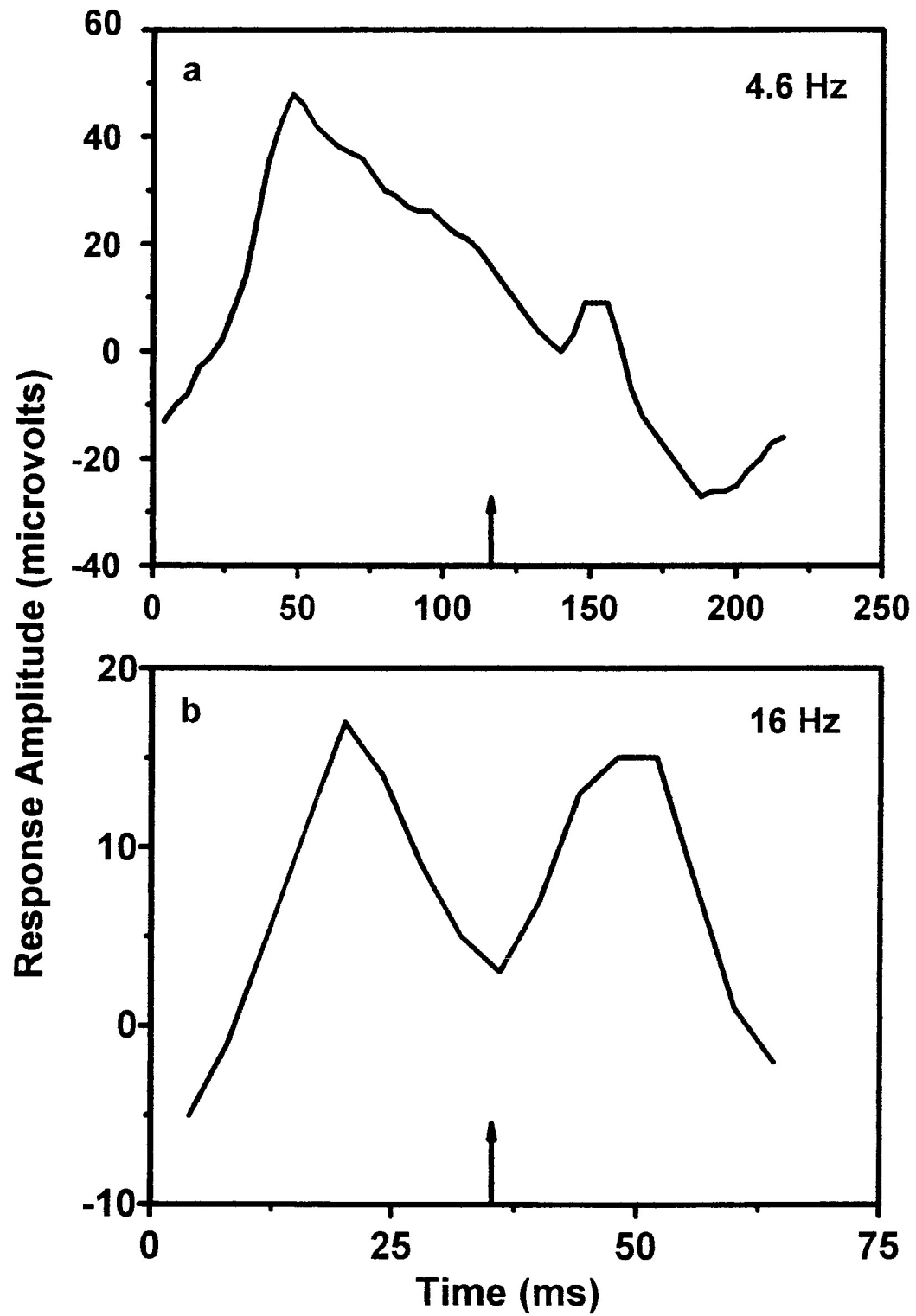






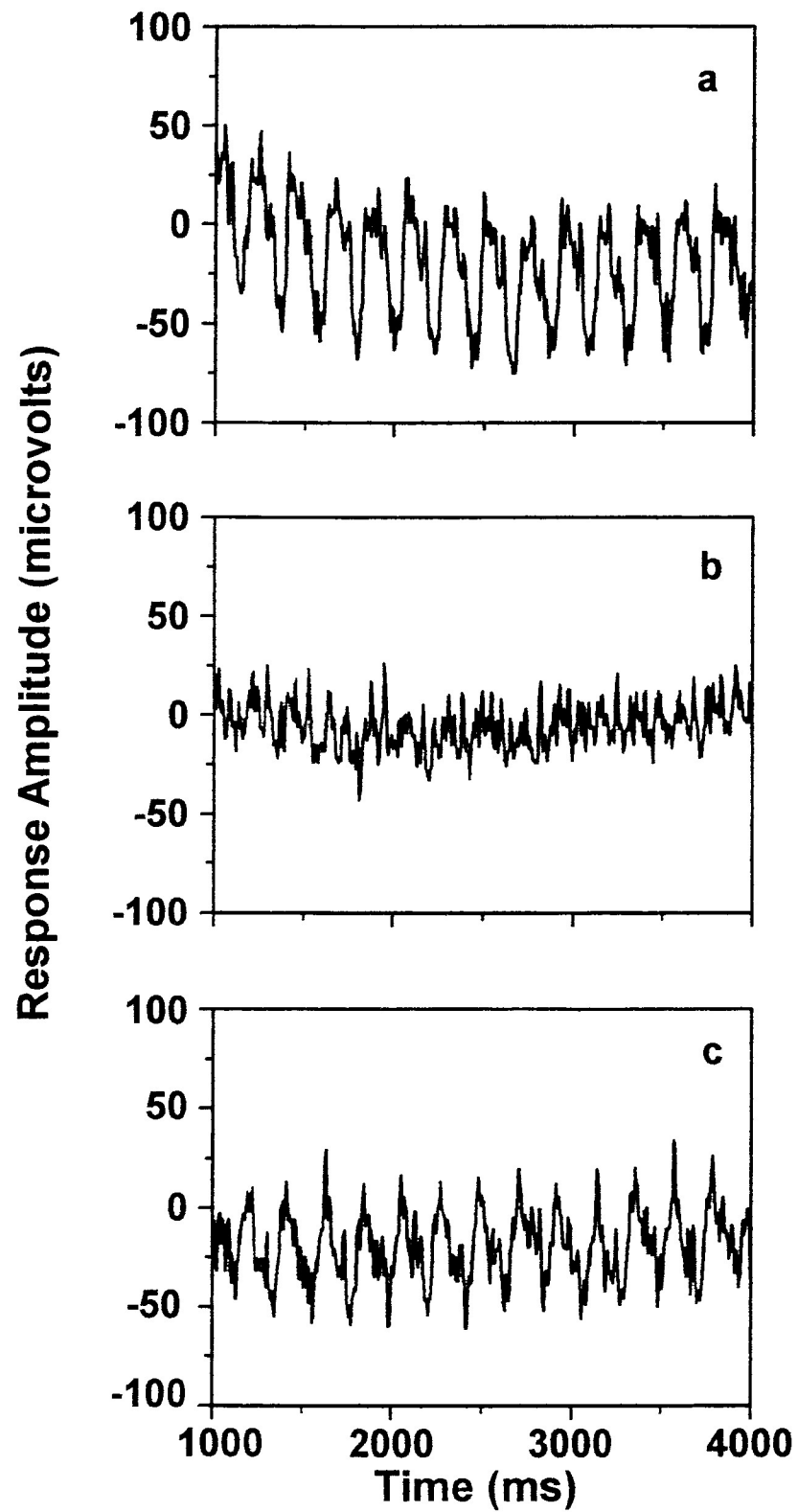
## Averaged ERG Responses to Flicker

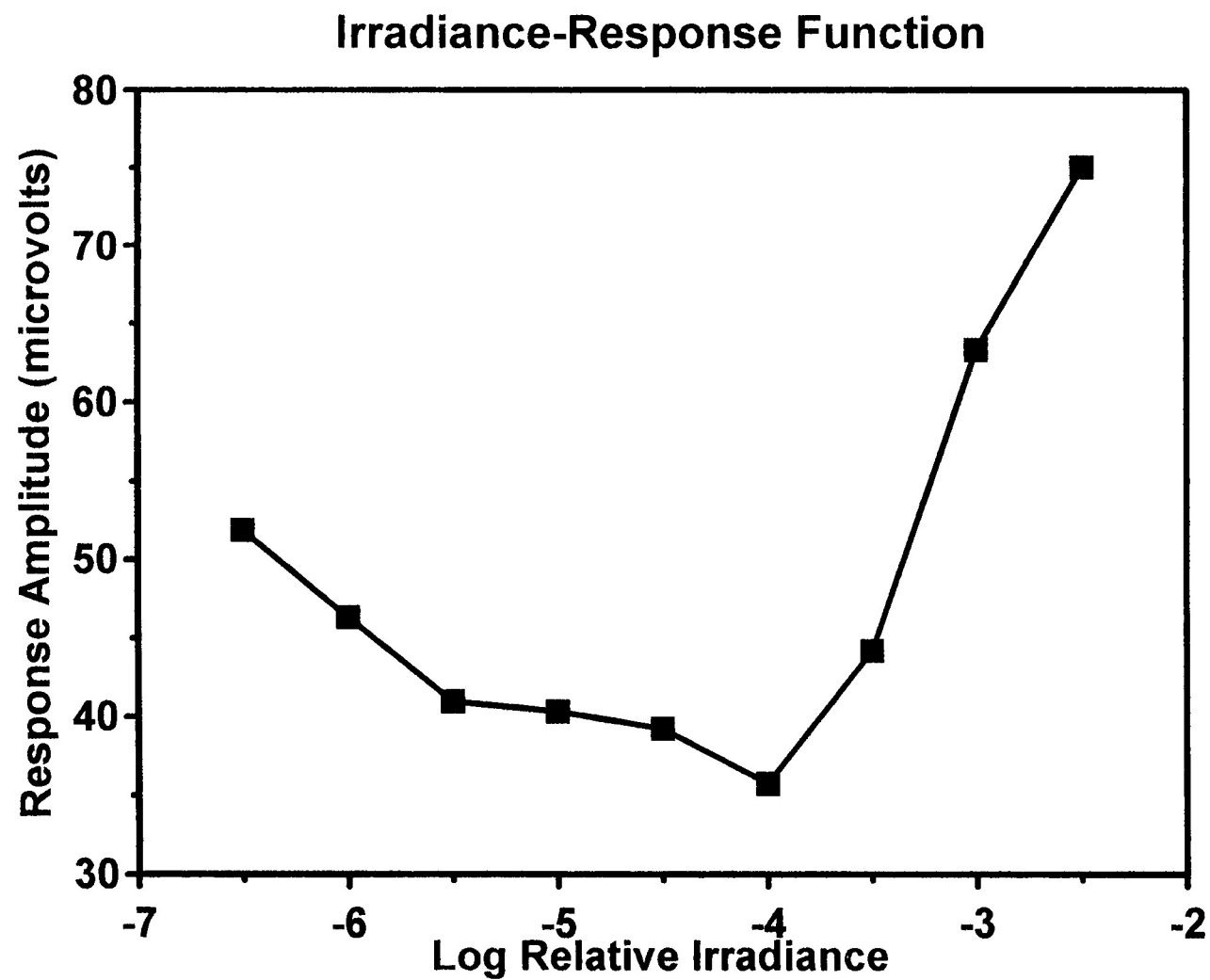
77

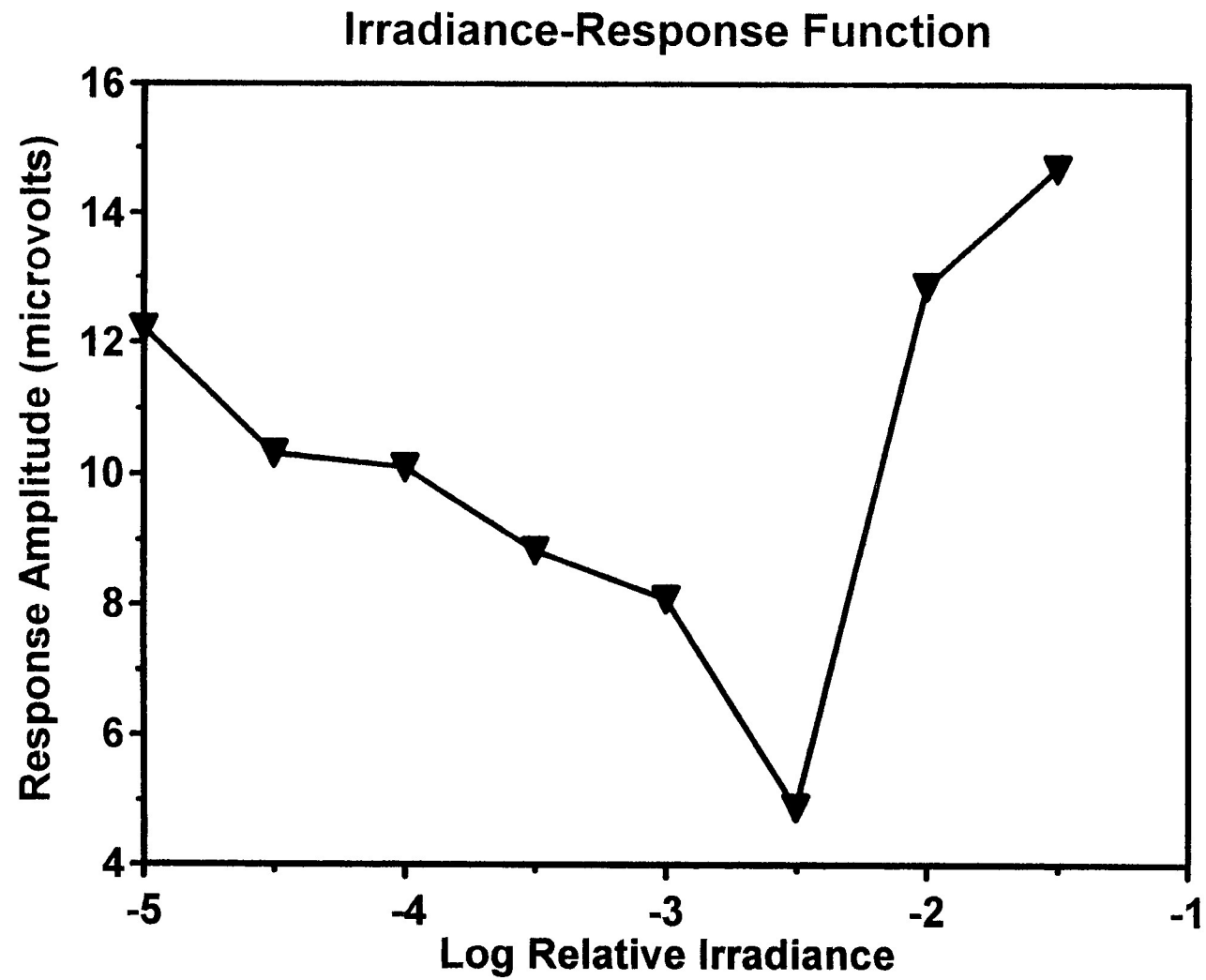


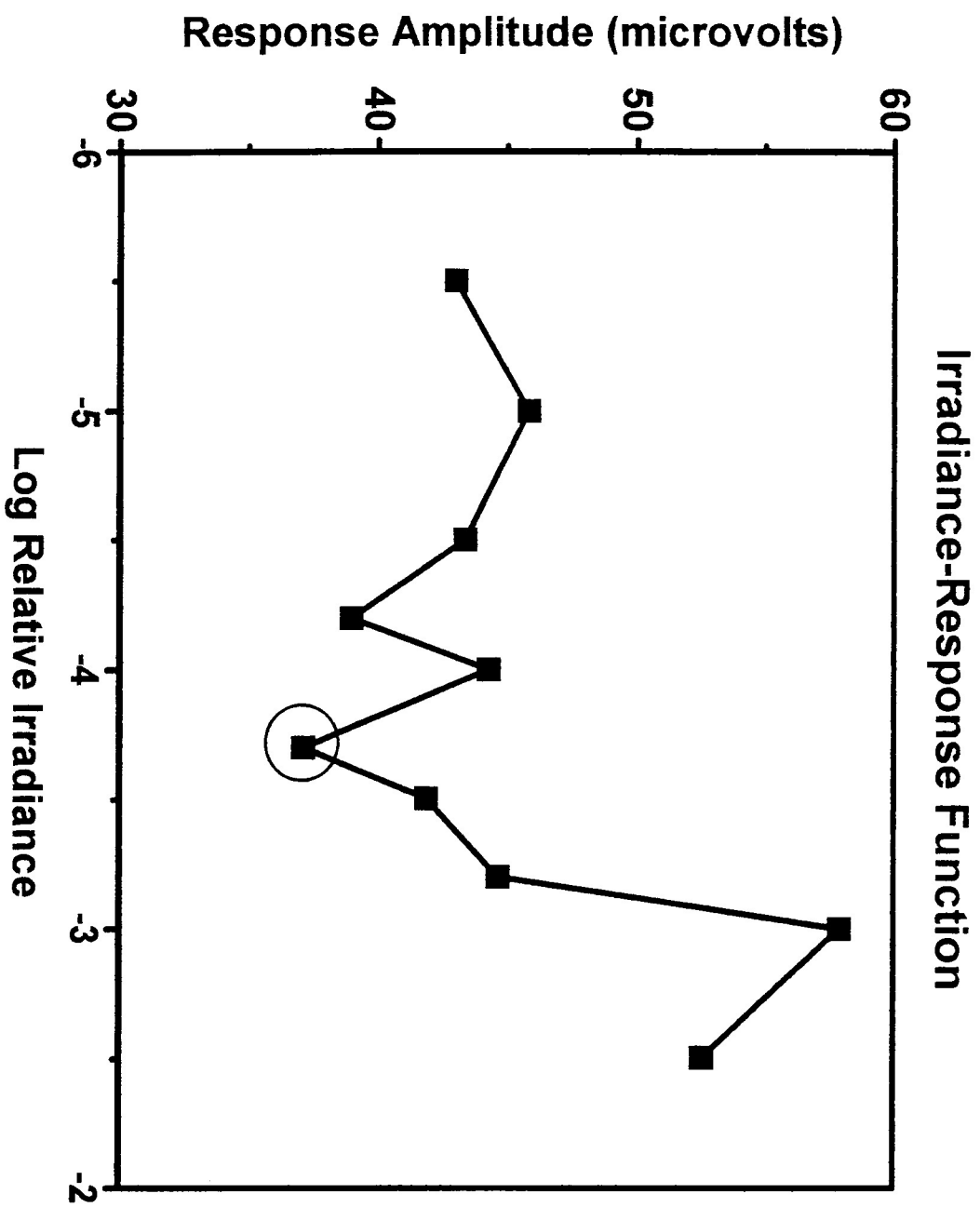
## ERG Responses to 4.6 Hz Stimuli

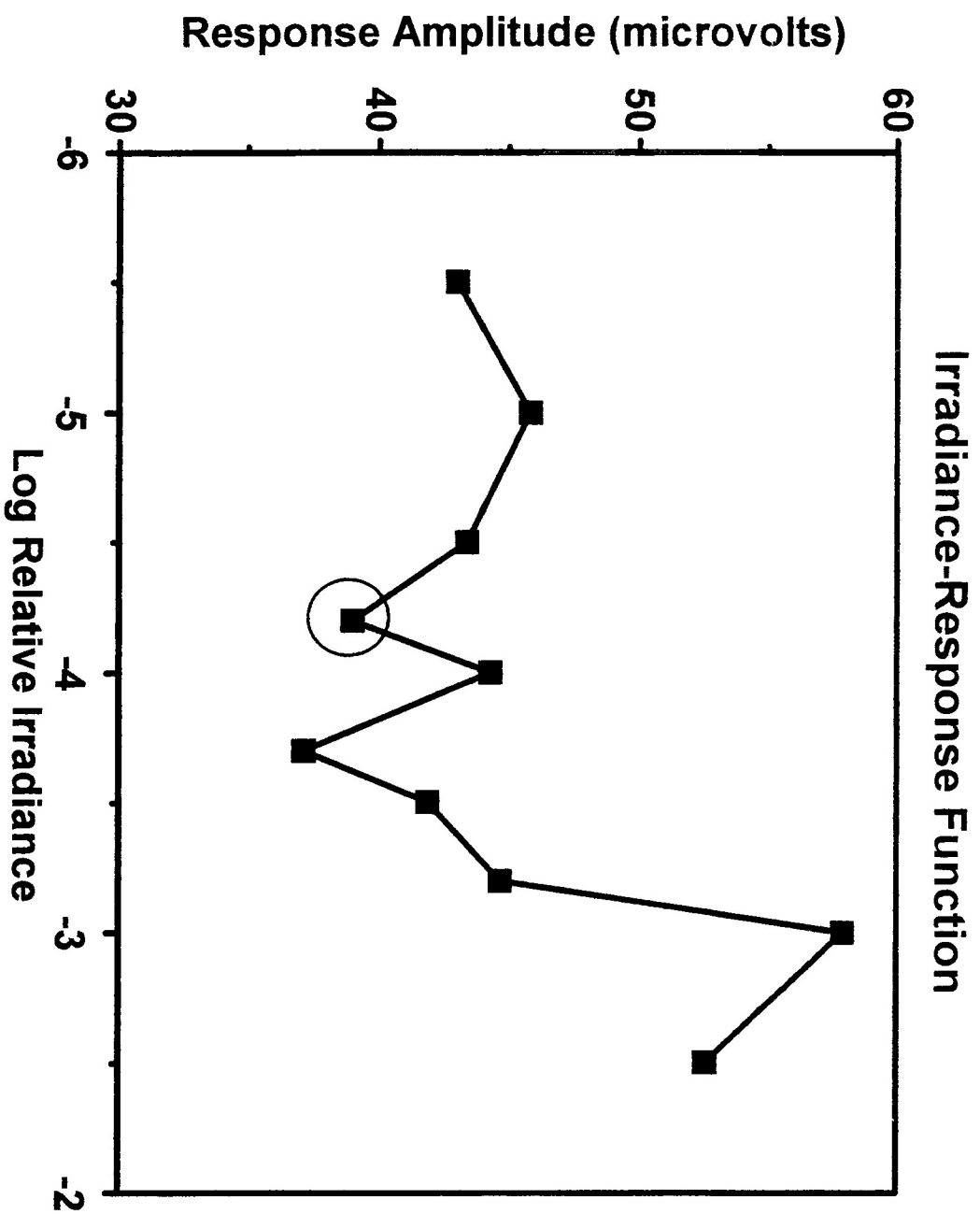
78



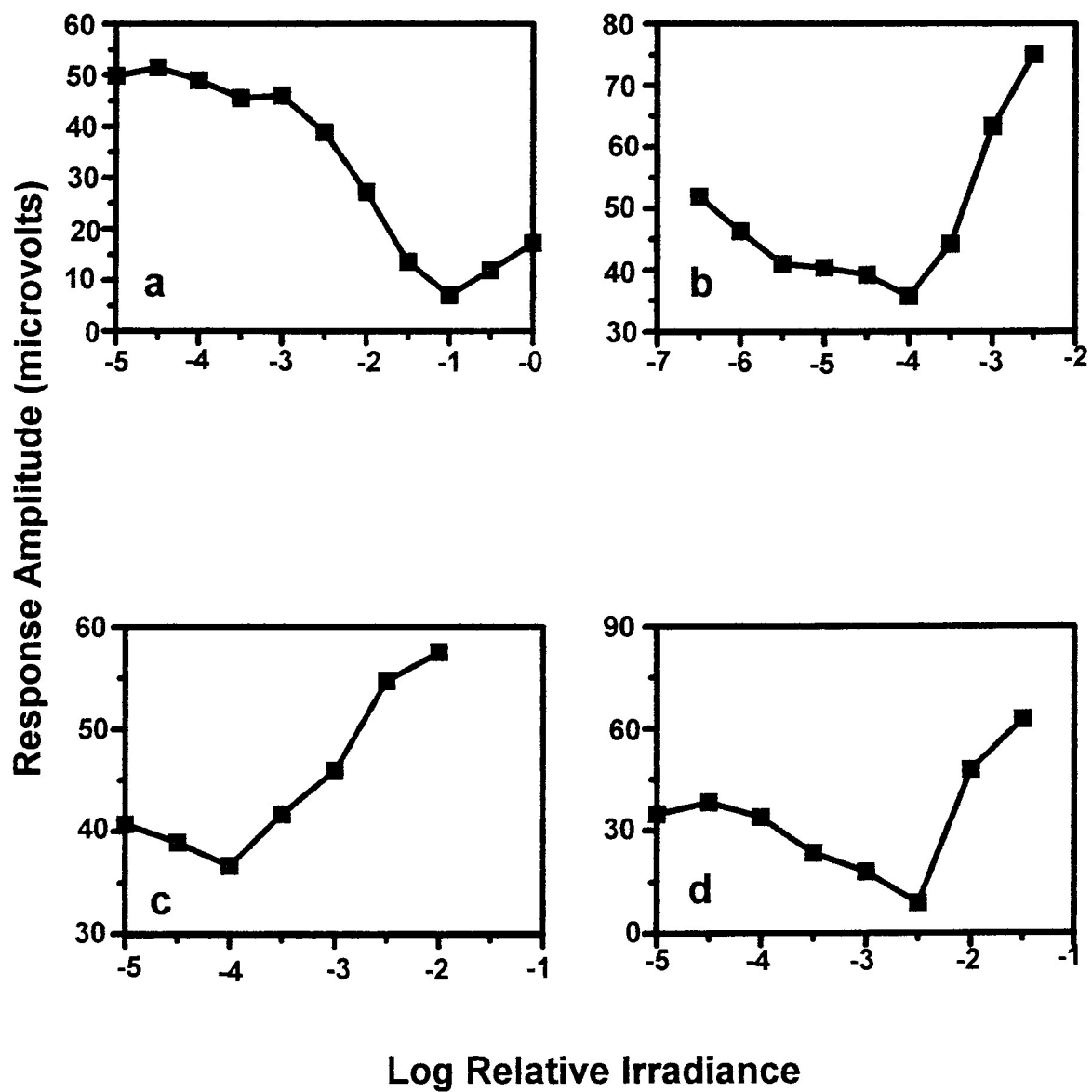


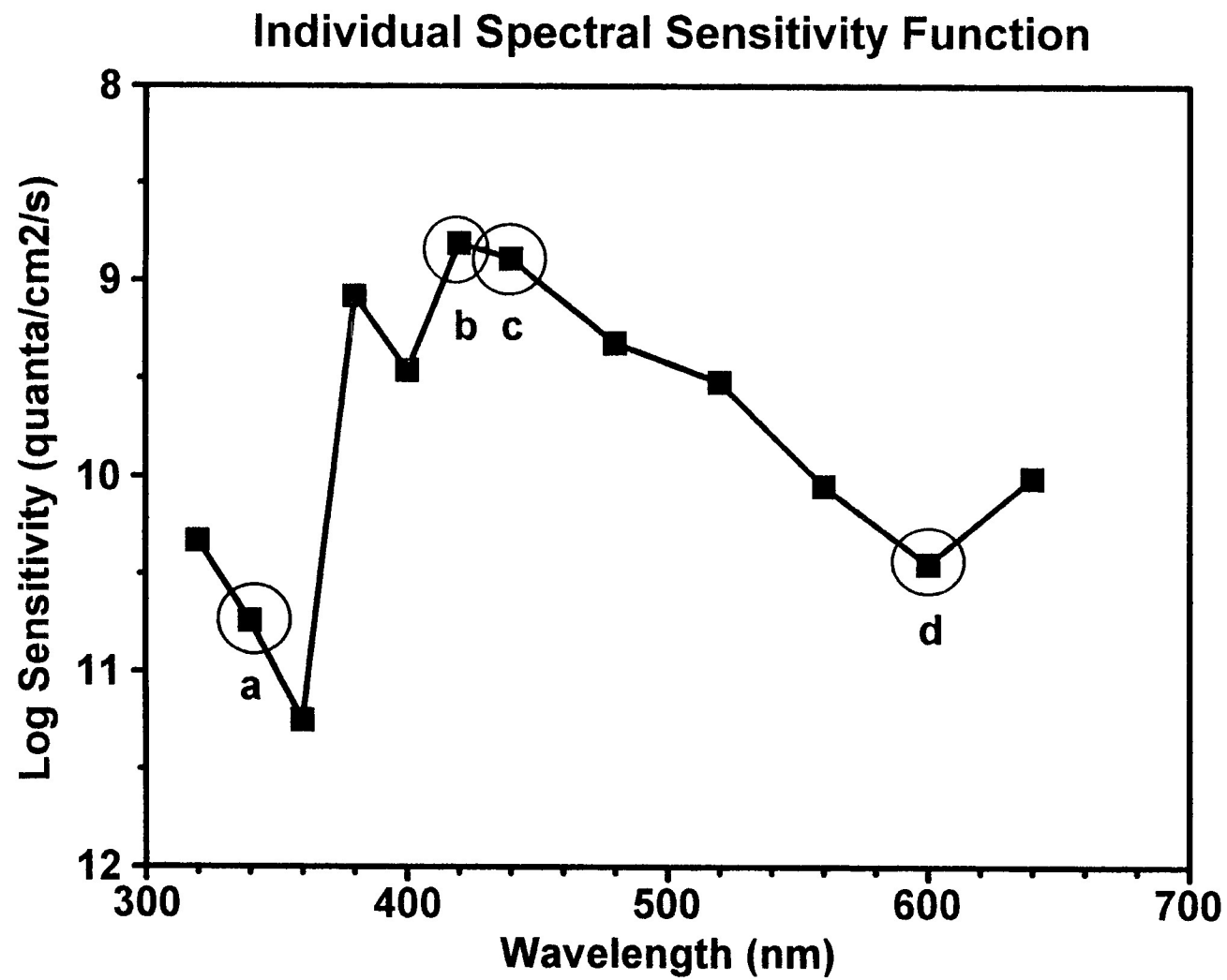




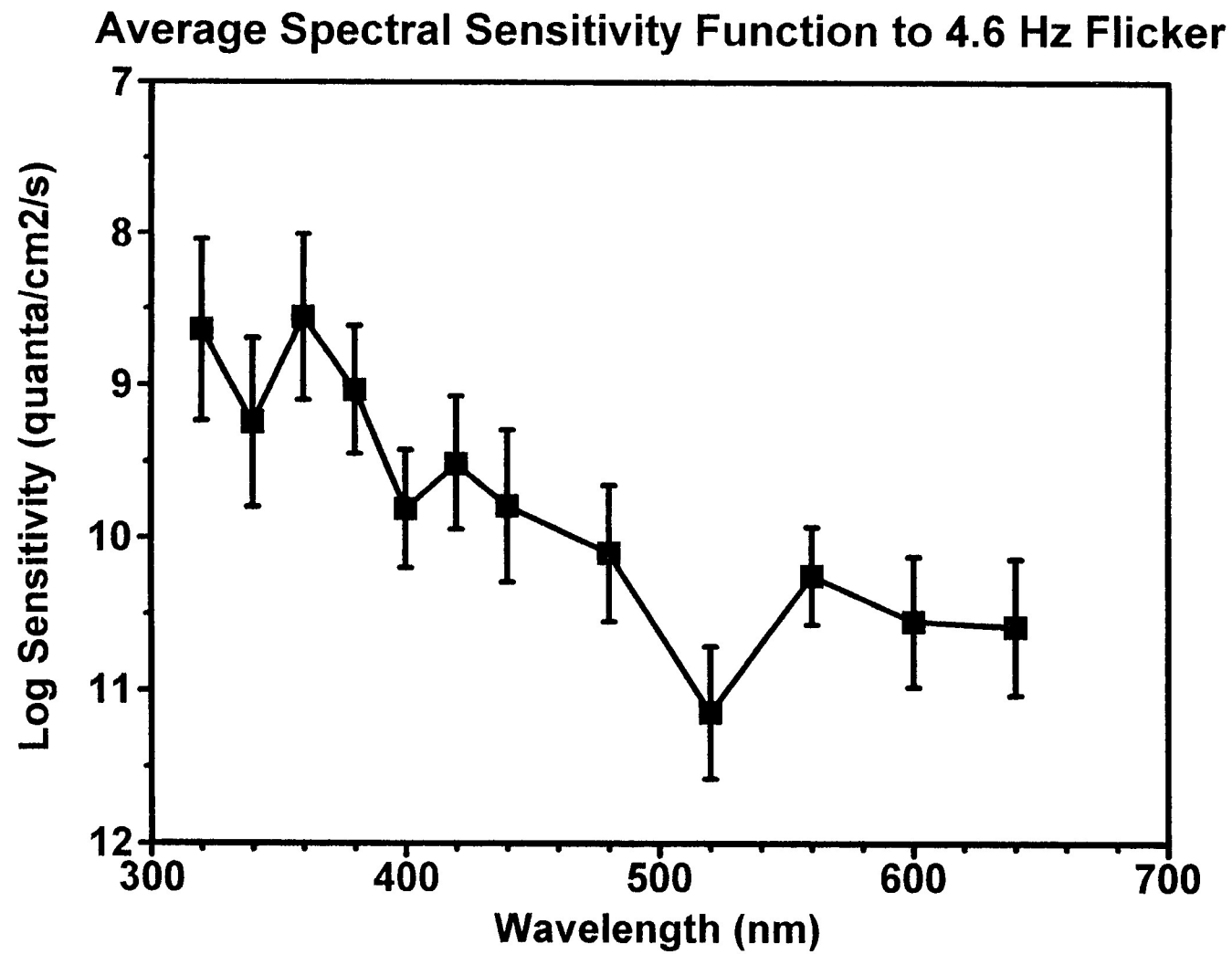


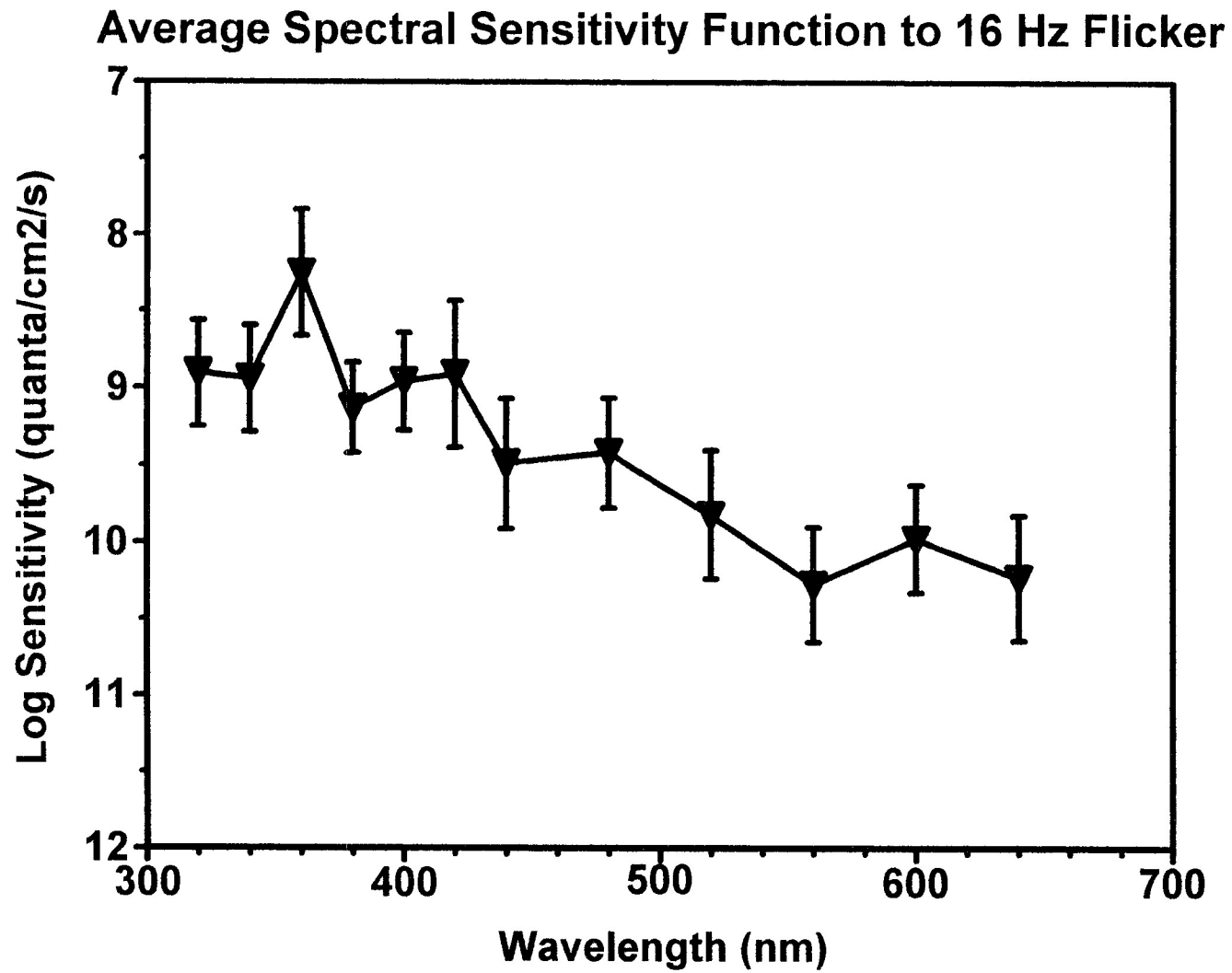
## Irradiance-Response Functions at Four Wavelengths

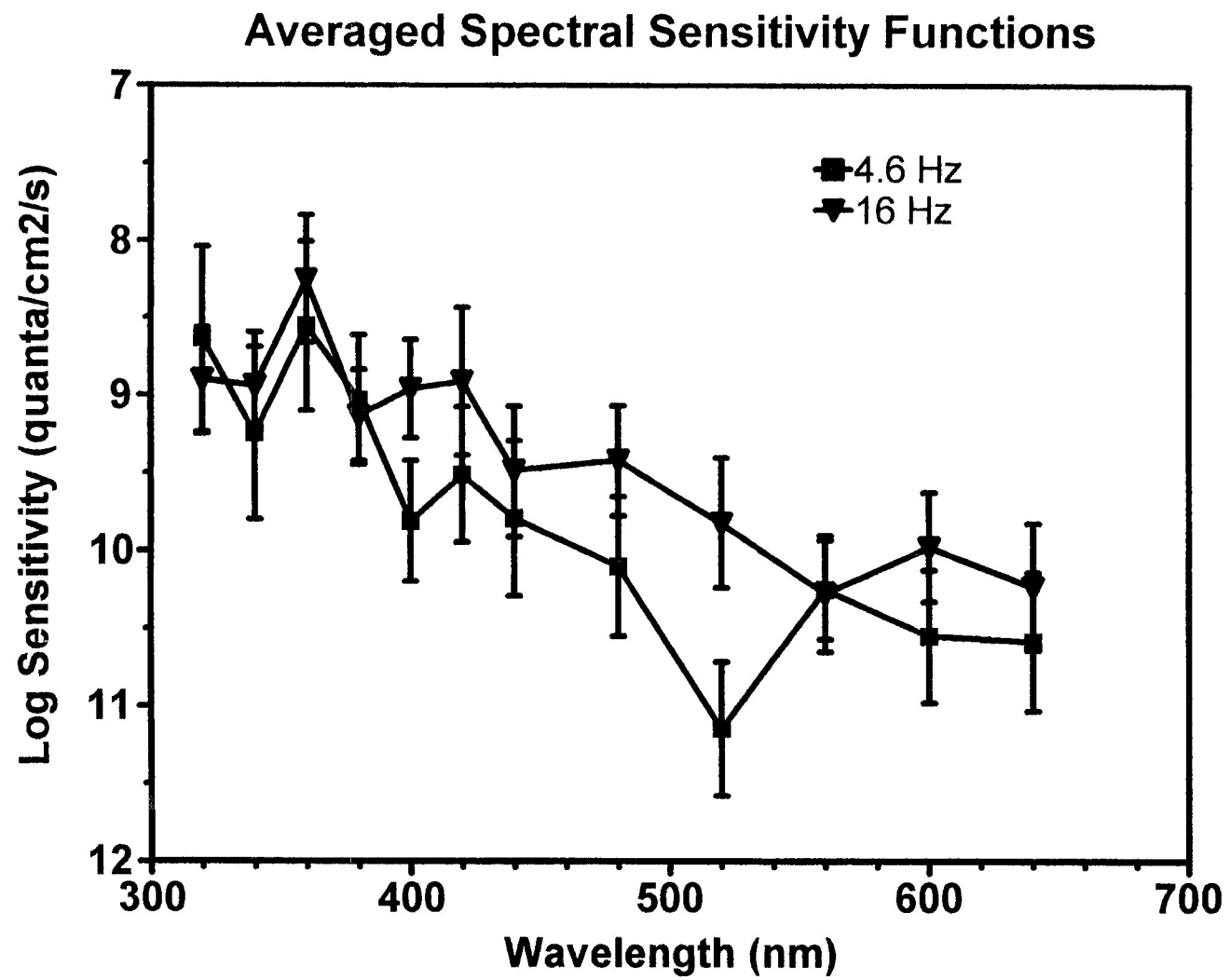




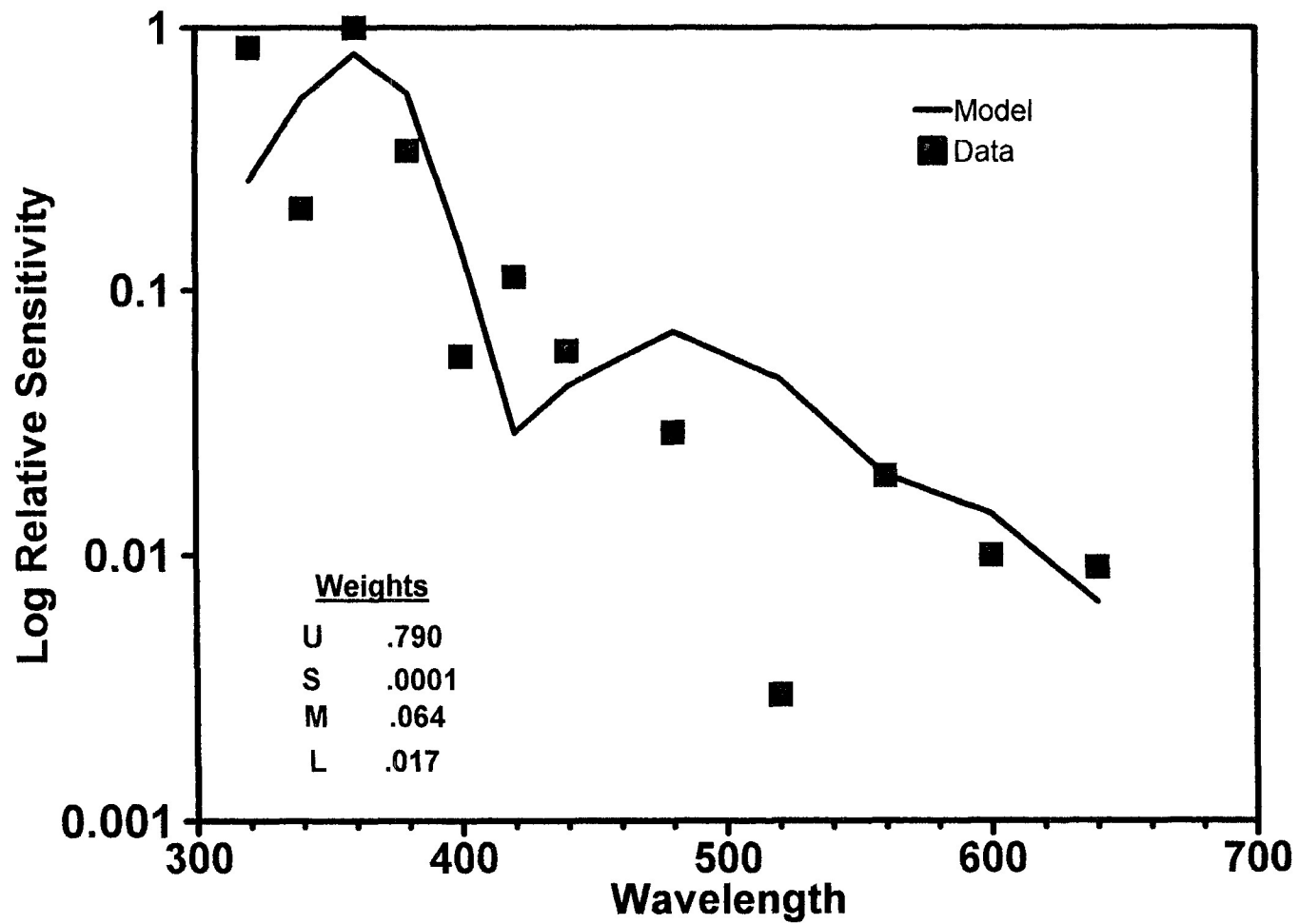




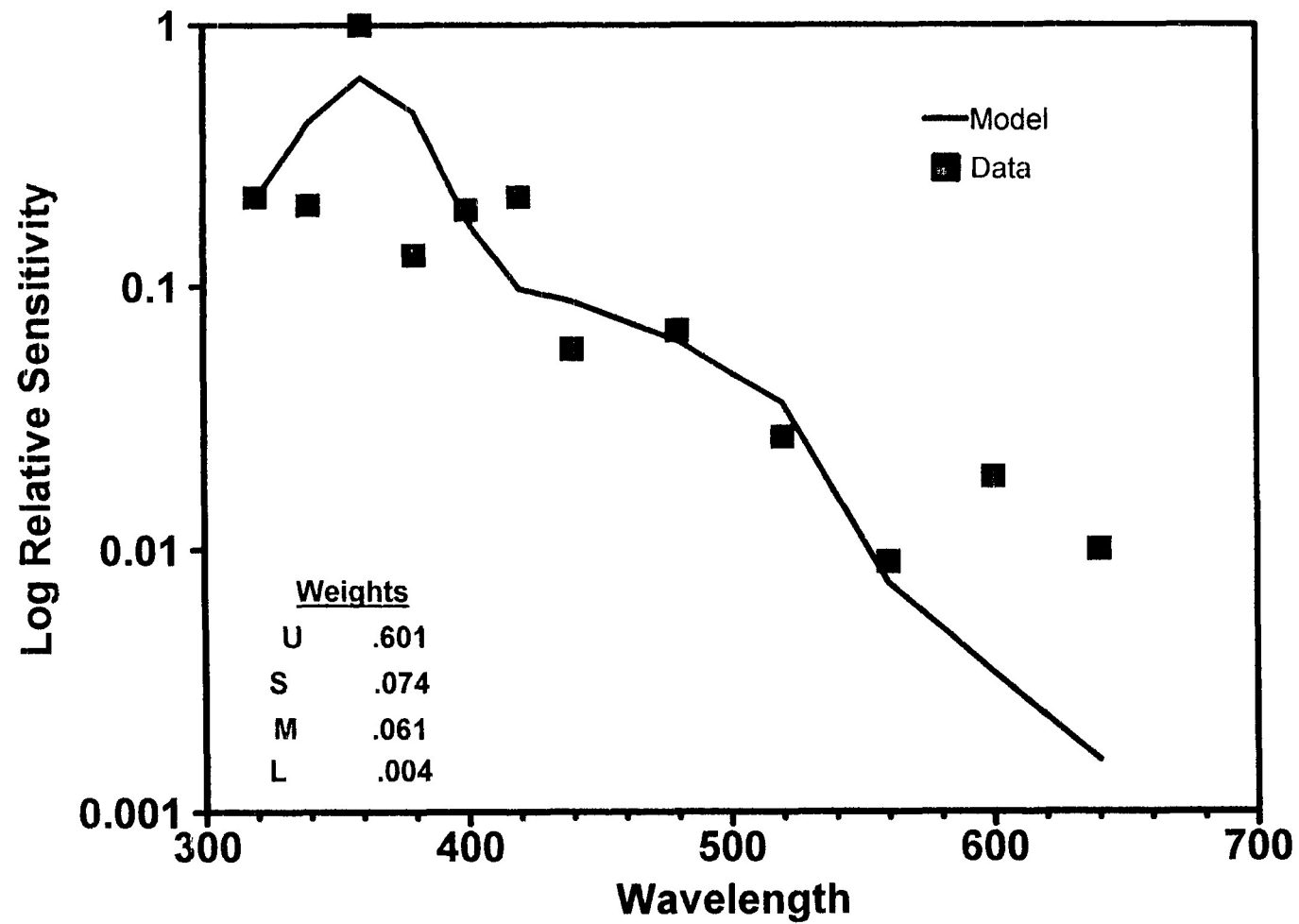




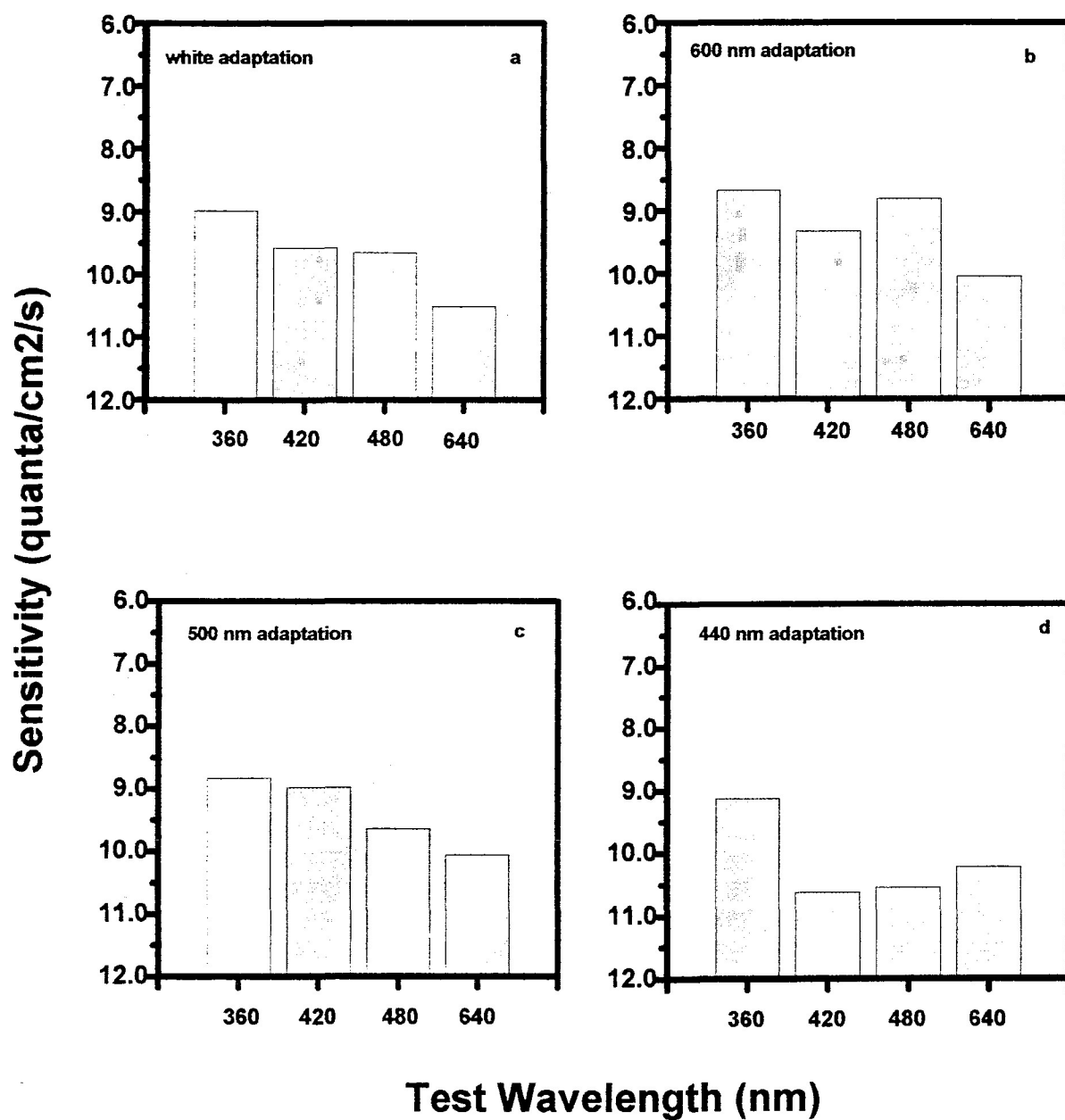
## Modeled Spectral Sensitivity Function to 4.6 Hz Flicker

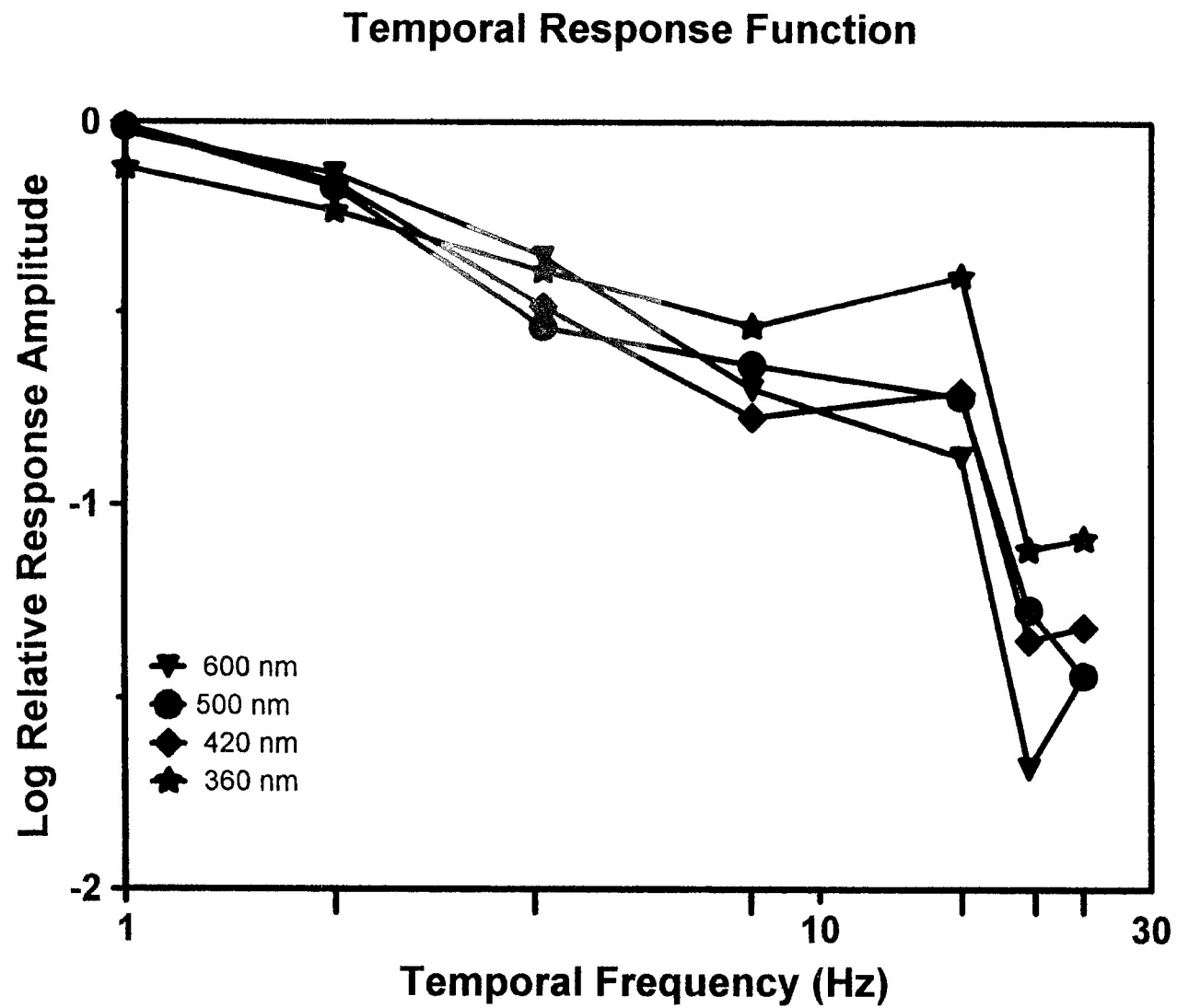


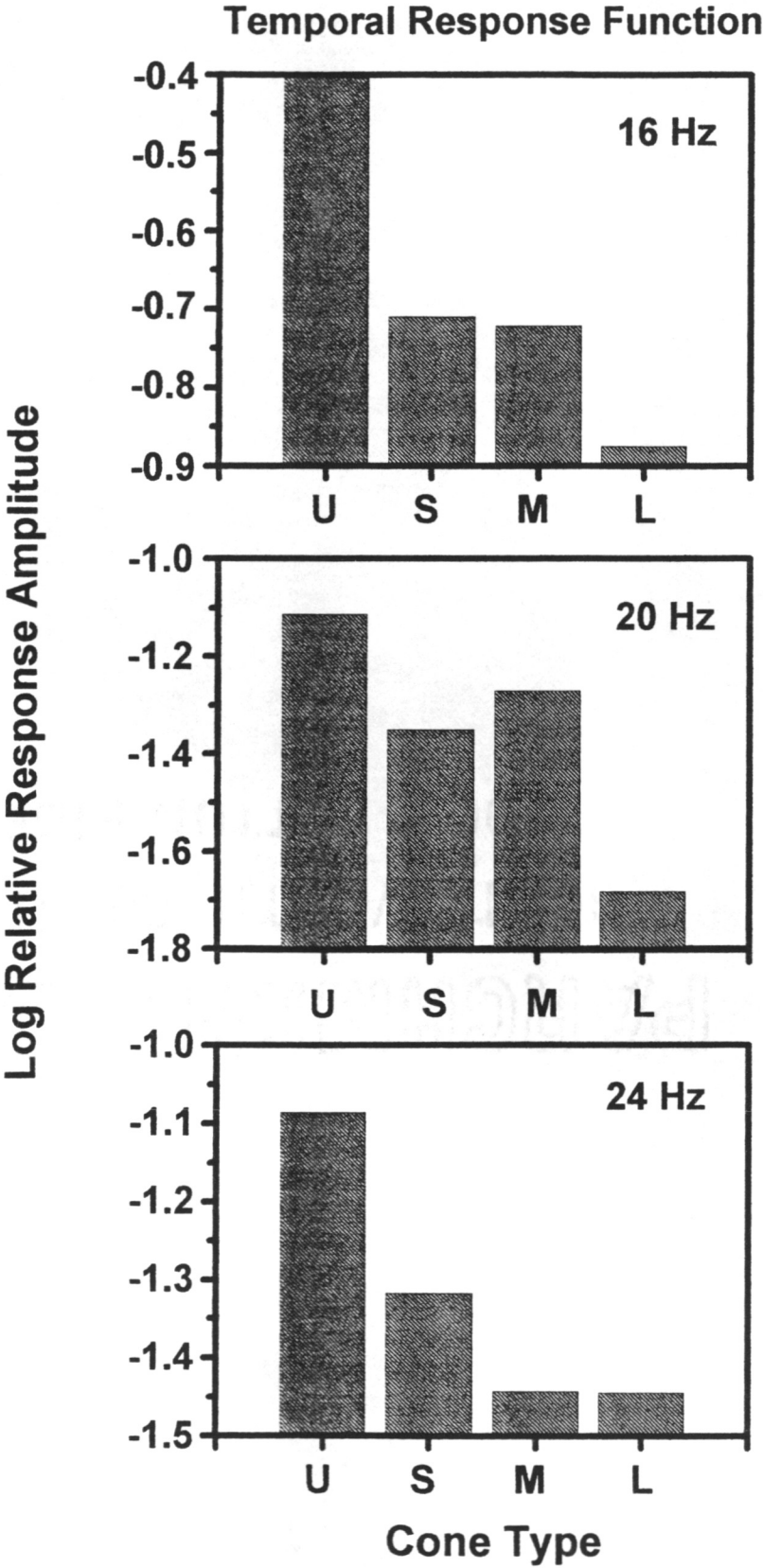
## Modeled Spectral Sensitivity Function to 16 Hz Flicker



## Response Suppression to Chromatic Adaptation









## Appendix

Log irradiance to each wavelength at 0.0 attenuation measured in quanta/cm<sup>2</sup>/s.

---

| Wavelength | Irradiance |
|------------|------------|
| 320        | 11.33      |
| 340        | 11.74      |
| 360        | 11.75      |
| 380        | 12.08      |
| 400        | 12.46      |
| 420        | 12.81      |
| 440        | 12.89      |
| 480        | 13.02      |
| 520        | 13.02      |
| 560        | 13.05      |
| 600        | 12.95      |
| 640        | 13.01      |

---

---